

1-1-1986

# Stopping theories and their influence on damage energy calculations

Uner Colak  
*Iowa State University*

Follow this and additional works at: <https://lib.dr.iastate.edu/rtd>

 Part of the [Engineering Commons](#)

## Recommended Citation

Colak, Uner, "Stopping theories and their influence on damage energy calculations" (1986). *Retrospective Theses and Dissertations*. 17383.  
<https://lib.dr.iastate.edu/rtd/17383>

This Thesis is brought to you for free and open access by the Iowa State University Capstones, Theses and Dissertations at Iowa State University Digital Repository. It has been accepted for inclusion in Retrospective Theses and Dissertations by an authorized administrator of Iowa State University Digital Repository. For more information, please contact [digirep@iastate.edu](mailto:digirep@iastate.edu).

Stopping theories and their influence  
on damage energy calculations

by

Uner Colak

A Thesis Submitted to the  
Graduate Faculty in Partial Fulfillment of the  
Requirements for the Degree of  
MASTER OF SCIENCE

Major: Nuclear Engineering

Signatures have been redacted for privacy

---

Iowa State University  
Ames, Iowa

1986

## TABLE OF CONTENTS

	PAGE
LIST OF SYMBOLS . . . . .	v
INTRODUCTION . . . . .	1
LITERATURE REVIEW . . . . .	5
DISPLACEMENT RADIATION DAMAGE . . . . .	9
STOPPING OF ENERGETIC IONS IN MATTER . . . . .	24
Nuclear Stopping . . . . .	26
Electronic Stopping . . . . .	36
RESULTS: DAMAGE ENERGY CALCULATIONS . . . . .	51
SUMMARY AND CONCLUSIONS . . . . .	67
BIBLIOGRAPHY . . . . .	71
ACKNOWLEDGMENTS . . . . .	75

## LIST OF TABLES

	PAGE
TABLE 1. Damage energies for copper PKAs in copper for the Firsov theory . . . . .	55
TABLE 2. Damage energies for copper PKAs in copper for the Brandt theory . . . . .	59
TABLE 3. Damage energies for copper PKAs in copper for the LSS theory . . . . .	60
TABLE 4. Damage energies for copper PKAs in copper calculated based on LSS, Firsov, and Brandt electronic stopping theories . . . . .	62
TABLE 5. Damage efficiencies calculated based on LSS, Firsov, and Brandt electronic stopping theories . . . . .	64



## LIST OF FIGURES

	PAGE
FIGURE 1. The $g(\varepsilon)$ function of Lindhard and the numerical approximation by Robinson . . . . .	18
FIGURE 2. Damage efficiencies as a function of PKA energy according to LSS theory . . . . .	19
FIGURE 3. The reduced nuclear stopping cross sections for Bohr, Molière, and LSS potentials . . . . .	35
FIGURE 4. Variation of potential with separation distance for a Cu-Cu interaction according to Coulomb, Bohr, LSS, Molière, and semiempirical Wilson potentials . . . . .	37
FIGURE 5. Ionization curve for heavy ions with velocity stripping parameter $b=1.33$ . . . . .	49
FIGURE 6. Electronic stopping power of copper for copper ions based on the LSS, Firsov, and Brandt theories . . . . .	53
FIGURE 7. Variation of damage energies with the initial energy of PKA based on LSS, Firsov, and Brandt electronic stopping theories . . . . .	63
FIGURE 8. Variation of damage efficiencies with the initial energy of PKA based on LSS, Firsov, and Brandt electronic stopping theories . . . . .	65

## LIST OF SYMBOLS

a	Screening length
$a_0$	Bohr radius ( $= \hbar^2/e^2 m = 0.529 \times 10^{-9}$ cm)
$a_B$	Bohr screening length (e.g., equation (37))
$a_L$	LSS screening length (e.g., equation (8))
$a_M$	Moliere screening length (e.g., equation (51))
$A_1$	Atomic mass number of projectile atom
$A_2$	Atomic mass number of target atom
$A_C$	Common atomic mass number for $A_1=A_2$
$b_i$	Constant coefficient of Molière and Wilson potentials
B	Beta function (e.g., equation (51))
$C(p_F)$	Material dependent constant in the expression for effective charge fraction (e.g., equation (74))
$C_i$	Constant coefficients of Molière and Wilson potentials
$-dT/dx$	Stopping power
e	Charge of electron ( $e^2=1.44 \times 10^{-13}$ MeV cm)
E	Energy of primary irradiating particle
$f(v_F)$	Scattering function in the expression for proton stopping
$f_{ENR}$	Echenique-Nieminen-Ritchie scattering function
$f_{LW}$	Lindhard-Winther scattering function
$f(r)$	Function in the expression for scattering angle (e.g., equation (26))
$f(t^{1/2})$	LSS scaling function (e.g., equation (12))
$g(\epsilon)$	Fitting function for calculation of damage energy (e.g., equation (16))

$h$	Planck's constant ( $= 4.136 \times 10^{-15}$ MeV sec)
$\hbar$	$h/2\pi$
$k_B$	Brandt electronic stopping cross section proportionality constant (e.g., equation (89))
$k_F$	Firsov electronic stopping cross section proportionality constant (e.g., equation (85))
$k_L$	LSS electronic stopping cross section proportionality constant (e.g., equation (14))
$k_s$	Constant in the expression for LSS potential (e.g., equation (38))
$K_d$	Displacement production rate (e.g., equation (20))
$K_{de}$	Damage energy rate (e.g., equation (22))
$m$	Mass of electron
$m_p$	Mass of proton
$M_1$	Mass of projectile particle
$M_2$	Mass of target particle
$n$	Number of electrons bound to the nucleus at a given reduced velocity, $y_r$
$N$	Number of target atoms per unit volume
$p$	Impact parameter
$p_F$	Fermi momentum
$q$	Ionization fraction
$Q$	Energy transferred to target electrons
$Q_i$	Ionic charge number
$r$	Separation distance
$r_s$	Electron radius
$s$	Variable of LSS potential

$s_e$	Reduced electronic stopping cross section (e.g., equation (56))
$s_n$	Reduced nuclear stopping cross section (e.g., equation (45))
$S_e$	Electronic stopping cross section
$S_{e,B}$	Brandt electronic stopping cross section (e.g., equation (75))
$S_{e,F}$	Firsov electronic stopping cross section (e.g., equation (54))
$S_{e,L}$	LSS electronic stopping cross section (e.g., equation (63))
$S_n$	Nuclear stopping cross section (e.g., equation (48))
$T$	Energy of the primary knock-on atom
$T'$	Energy transferred to target nucleus
$T_d$	Displacement threshold energy
$T_I$	Ionization cutoff energy
$T_L$	Energy scaling quantity (e.g., equation (7))
$T_m^{\dagger}$	Maximum transferred energy
$U$	Binding energy of atoms
$U_i$	Ionization energy of electrons
$v$	Velocity of moving particle
$v_o$	Bohr velocity ( $= e^2/\hbar = 2.188 \times 10^8$ cm/sec)
$v_1$	Upper velocity limit for the validity of LSS and Firsov theories
$v_e$	Velocity of conduction electrons (e.g., equation (68))
$v_F$	Fermi velocity (e.g., equation (69))
$v_r$	Velocity of moving ion relative to the conduction electrons of the medium (e.g., equation (71))

V	Potential energy
x	Traveled path length
$y_r$	Reduced velocity (e.g., equation (72))
Z	Function in the expression for k (e.g., equation (15))
$Z_1$	Charge number of projectile atom
$Z_2$	Charge number of target atom
$(Z_1)^*$	Effective charge number
$Z_c$	Common charge number for $Z_1=Z_2$
$\alpha$	Variable of the equation for relative velocity (e.g., equation 71))
$\beta$	Constant of LSS screening length, $(9\pi^2/128)^{1/3}$
$\phi$	Flux
$\phi(r/a)$	Screening function (e.g., equation (35))
$\phi'_E$	Differential flux with respect to energy E
$\varepsilon$	Reduced energy (e.g., equation (9))
$\lambda$	Constant in the expression for $f(t^{1/2})$ (e.g., equation (12))
$\Lambda$	Brandt screening length (e.g. equation (73))
$\kappa$	Correction coefficient to multiplication factor due to forward scattering
$\omega$	Variable in the expression for $f_{LW}$ (e.g., (78))
$\rho$	Distance of closest approach
$\rho_0$	Distance of closest approach in a head-on collision for the Coulomb potential (e.g., equation (33))
$\rho_L$	Reduced range (e.g., equation (58))
$\gamma_s$	Variable in the expression for differential scattering cross section for LSS potential (e.g.,

equation (44))

- $\theta$  Scattering angle in the center-of-mass system  
(e.g., equation (25))
- $\sigma_d$  Displacement cross section (e.g., equation (18))
- $\sigma_{de}$  Damage energy cross section (e.g., equation (19))
- $\sigma'_t$  Reduced differential scattering cross section with  
respect to  $t$  (e.g., equation (11))
- $\sigma'_T$  Differential scattering cross section with respect  
to  $T$  (e.g., equation (19))
- $\sigma'_{T'}$  Differential scattering cross section with respect  
to  $T'$  (e.g., equation (6))
- $\xi$  Coefficient in the expression of LSS electronic  
stopping cross section (e.g., equation (54))
- $\nu$  Multiplication factor (e.g., equation (1))
- $\zeta$  Effective charge fraction (e.g., equation (74))

## INTRODUCTION

Advances in the field of radiation effects on materials have yielded a better understanding of the nature of materials, as well as providing basic information for the development of commercial use of nuclear energy. Basic theory of point defect production by irradiation has allowed important insights into mechanisms on the atomic scale that determine mechanical and physical property changes of materials under irradiation conditions.

The nature of irradiation effects on materials primarily depends on the type of irradiating particle (such as neutron or charged particle), irradiation time and temperature, energy of incident particle, and target material. Neutron irradiation has a special importance from the technological point of view. On the other hand, it is more convenient to produce similar effects by charged particle irradiations using accelerators than by neutron irradiation using nuclear reactors. Recently, high and medium energy proton accelerators have been used to simulate the radiation damage produced in controlled thermonuclear reactor environments [1,2]. Technological applications of charged particle irradiations such, as material analysis and ion implantation, have increased the attention to radiation effect analysis for charged particles.

The basic damage production mechanism in metals is associated with the displacements of atoms from their regular lattice sites. An understanding of the slowing-down mechanism of energetic particles in solids is basic to the prediction of the number of displacements produced by the incident particle.

Knowledge about the energy partition between nuclei and electrons during the slowing-down of the struck atom is of primary importance to the radiation damage process. Many theories have been proposed for the separate nuclear and electronic energy loss mechanisms. Due to the complexity of this slowing-down process, none of the theories gives an exact description of the energy loss. Experimental observation of energy loss processes has been focused on light ions and fission fragments. In the radiation damage studies, energy loss of heavy ions has a special importance. One of the basic theories on the stopping of heavy ions was proposed by Lindhard et al. [3,4,5]. They developed a comprehensive approximation method for screened Coulomb fields starting with Bohr's suggestions [6]. They also described and used dimensionless quantities for the basic parameters, such as incident energy, transferred energy, stopping power, and range. This theory, also known as LSS theory, has been widely used in radiation damage calculations. An alternative method for analyzing the



stopping of energetic ions was proposed by Firsov [7,8]. Firsov's theory has been used especially for the determination of energy loss of particles in crystalline materials. Recently, promising advances for the energy loss of heavy ions were proposed by Brandt and Kitagawa [9] and Brandt [10]. Their work concentrated on the influence of effective charge states as a function of the velocity of the slowing ion. Their calculations for heavy ions are shown to be consistent with observations for protons.

In this work, basic stopping theories relevant to radiation damage studies are reviewed. Special attention is paid to the LSS, Firsov, and Brandt theories. The effect of these stopping theories on the radiation damage calculations is analyzed. This analysis is done for a copper target, which has been widely investigated in radiation damage studies. A computer program is developed to calculate the damage energy, a part of the energy of the primary knock-on atom which is used for collision cascade formation. Damage energies are evaluated by means of the electronic stopping parameters of the LSS, Firsov, and Brandt theories, while the nuclear stopping parameters are used according to LSS theory. Crystalline structure of target material and temperature effects are not considered. Channeling and focusing due to crystalline structure and migration and

recombination of defects due to thermal activation should be considered in future work.

## LITERATURE REVIEW

Beginning with reactor studies of nuclear energy, radiation effects became an important subject. Interactions of energetic particles with solids and effects of lattice defects on the properties of solids have been the primary interest of many investigators.

The first displacement cascade theory for random collisions was developed by Kinchin and Pease [11]. They determined the number of displaced atoms considering hard-sphere elastic scattering. Electronic energy loss, i.e., energy transferred to the target electrons, was not taken into account in this theory.

Lindhard et al. [3] analyzed the distribution of transferred energy between nuclei and electrons during the slowing-down of ions. They realistically approached the problem and developed the damage energy concept, which focuses on the energy available for displacement production. Later, the simple theory of Kinchin and Pease was extended using damage energies [12,13]. This modified displacement cascade theory has been suggested as a standard procedure for radiation damage calculations [14].

Calculation of damage energies requires a knowledge of the energy partition between target atoms and electrons during slowing-down of energetic particles in matter. Theoretical and experimental studies of the stopping of ions

in matter were started during the early years of this century. Early investigations have been accomplished for high energy particles in atomic structure studies.

Theoretical treatments of the stopping of charged particles were founded by Bohr [6] and Bethe [15].

A quantum mechanical treatment of stopping theory was developed by Bethe [15]. This theory is based on the plane-wave approximation of Born. Then, Bloch restated the basic parts of Bethe's theory by use of an impact parameter treatment [16]. Application of this Bethe-Bloch formalism is limited to the high velocity region. The theory fails for slow particles.

For the studies of radiation effects on materials, the low energy aspect of stopping theory received considerable attention. The first stopping theory relevant to radiation damage studies was introduced by Bohr [6]. He analyzed the scattering phenomena for unscreened and screened Coulomb fields by a classical mechanical treatment. He separated the total energy loss of ions into two components, nuclear and electronic energy loss. Bohr also investigated the capture and loss properties of electrons in atomic collisions. This is one of the important antecedents of charge state theory for partially stripped ions.

In the late fifties and early sixties, theoretical work has focused on low energy particles. Lindhard and coworkers

extensively studied the screened Coulomb fields for the Thomas-Fermi atom model based on Bohr's suggestions [4,5]. They considered electronic and nuclear collisions separately and developed a statistical approach to the energy loss of low and intermediate energy ions. Firsov considered the same problem with somewhat different parameters [7,8]. He used numerical techniques to evaluate the interatomic potential for two Thomas-Fermi atoms. Both Lindhard's and Firsov's theories predict stopping power proportional to velocity for the low velocity region.

Experimental results showed that the atomic number of the target atom  $Z_2$  and incident ion  $Z_1$  could affect the stopping power [17]. These effects are known as  $Z_1$  and  $Z_2$  oscillations. Theories of Lindhard and Firsov do not consider such oscillations [18].

Some correction factors to the Bethe-Bloch equation have been suggested for fast ions [19,20]. These factors are known as shell and density corrections, and they are especially important at velocities close to those for maximum stopping power, as well as at relativistic velocities.

During the last decade, experimental results were used to generate semiempirical relations [21,22]. Recently, Brandt and Kitagawa made advances in stopping theory [9]. They calculated stopping powers for heavy ions by using the

concept of effective charge states. They determined the effective charge of partially stripped ions by considering the velocity of the projectile relative to the Fermi velocity of the target material.

Existing stopping theories allow us to determine stopping powers with an average accuracy of better than 10% for low velocity heavy ions and better than 2% for high velocity light ions [23]. Only a few of these theories are applicable to radiation damage calculations. LSS theory has been widely used for this purpose [24,25]. Firsov's theory has been applied to the calculation of radiation damage parameters in crystalline materials [26]. Brandt's theory may be utilized for heavy ion energy loss calculations in radiation damage studies as an alternative approach.

To analyze the influence of existing low energy electronic stopping theories on the radiation damage calculations, an important parameter, damage energy, which is the energy consumed for displacement production, is evaluated by using the parameters of these theories. Essentially, the number of displacements produced in a collision cascade is proportional to the damage energy. The accurate prediction of damage energies will provide a better understanding in the property change of materials due to irradiation.

## DISPLACEMENT RADIATION DAMAGE

An energetic incident particle (say, a 1 MeV neutron) can transfer to a lattice atom considerably more energy (thousands of eVs) than is required to displace the atom from its lattice site (tens of eVs). Thus, each primary collision can result in a cascade of secondary displacements as the primary struck atom partitions its energy to other atoms in secondary collisions. If energy transferred to target nucleus is much greater than the energy binding the atom to its lattice site, it is displaced from the regular site creating a vacancy and an interstitial, i.e., creating a displacement. Otherwise, this energy goes into thermal vibrations without any displacement. The target atom which is first struck and displaced by the incident particle is called a primary knock-on atom (PKA). After the collision, the PKA possesses kinetic energy and may be capable of producing more displacements by interacting with other lattice atoms. Displacement production proceeds until the energies of moving atoms fall below a certain energy, which is called the displacement threshold energy,  $T_d$ . The ensemble of displacements created by a single PKA is known as a displacement cascade. Transferred energy to target electrons,  $Q$ , results in excitation and ionization of electrons (hereafter, collectively called "ionization"). This energy does not contribute to the production of defects

in metals.

In the analysis of material behavior under irradiation conditions, it is necessary to know the displacement production rate and spatial distribution of displacements. The first theory for the estimation of the number of displaced atoms in a single cascade was introduced by Kinchin and Pease [11]. Their basic assumptions are:

1. All moving atoms lose their energies only by elastic collisions with nuclei, and no account is taken of the energy transferred to electrons.
2. Atoms behave like hard spheres in these collisions.
3. If a struck atom receives kinetic energy greater than the displacement threshold energy, it is displaced from its lattice site. Otherwise, it is not displaced.

Their conclusion may be represented by the following relations:

$$v(T) = \begin{cases} 0 & , \quad T < T_d \\ 1 & , \quad T_d \leq T < 2T_d \\ T/(2T_d) & , \quad 2T_d \leq T \end{cases} \quad (1)$$

where

$v(T)$  = multiplication factor, i.e., the number of displacements produced per PKA,



$T_d$  = displacement threshold energy,

$T$  = energy transferred to the PKA.

Since the Kinchin-Pease theory gives no consideration to the ionization of electrons, the number of displaced atoms is overestimated, especially for high values of  $T$ . The probability of transferring some of the energy  $T$  to the electrons increases with increasing  $T$ . In order to consider ionization losses, a crude correction was developed. The ionization cutoff energy is roughly approximated by [27]

$$T_I = A_2 \quad (2)$$

where  $T_I$  = ionization cutoff energy (keV),

$A_2$  = atomic number of target material.

In this approach, energy transfer is assumed to occur only by hard-sphere elastic scattering at transferred energies below  $T_I$ , and only by ionization above  $T_I$ .

The Kinchin-Pease model together with ionization corrections are represented by the following relation:

$$v(T) = \begin{cases} 0 & , \quad T < T_d \\ 1 & , \quad T_d \leq T < 2T_d \\ T/(2T_d) & , \quad 2T_d \leq T < T_I \\ T_I/(2T_d) & , \quad T_I \leq T \end{cases} \quad (3)$$

Robinson [28] and Sigmund [29] analyzed the Kinchin-Pease displacement model by inverse power scattering

(forward scattering) law instead of hard-sphere approximation (isotropic scattering). However, they excluded energy transfer to electrons. They represented their results as

$$v(T) = \kappa \frac{T}{2T_d}, \quad T > 2T_d \quad (4)$$

where the coefficient  $\kappa$  was determined by Sigmund [29] to be  $(12/\pi^2) \ln 2 = 0.84$ .

Lindhard et al. [3] showed that relative energy transfer to electrons as a continuous function of  $T$  could not be neglected even for low energy transfers. They developed a statistical model (LSS model) using the Thomas-Fermi atom model, and they also considered forward scattering [4,5]. The LSS model results in fewer displacements compared to hard-sphere scattering, since forward scattering yields a higher proportion of subthreshold collisions. Lindhard et al. estimated the number of displaced atoms as follows [3]. A particle moving in a material with energy  $T$  makes collisions with target atoms and their electrons. Collision events are described by the differential scattering cross section  $\sigma_T^i, dT'$  for energy transfers to target atom between  $T'$  and  $T'+dT'$ , where  $\sigma_T^i$  is a function of  $T$  and  $T'$ . Energy transferred to target

electrons is  $Q$ . After the collision, the incident particle energy is reduced from  $T$  to  $(T-T'-Q)$ , whereas the struck atom possesses the energy of  $(T'-U)$ .  $U$  is the binding energy of the struck target atom. Likewise, the energy of target electrons becomes  $(Q-U_i)$  where  $U_i$  is the sum of ionization energies of ionized electrons. The LSS theory is based on the following assumptions:

1. The struck electron moving through the solid does not produce displacements, because of its low mass.
2. Atomic binding energy  $U$  is neglected.  $U$  is of order of few eVs and low compared to the energy transferred to nuclei,  $T'$ .
3. Nuclear and electronic collisions are considered separately.
4. Energy transferred to nuclei,  $T'$ , is low compared to  $T$  since the scattering is forward peaked.
5.  $U_i$  is low compared to  $Q$ , and it is neglected.

Based on these assumptions, the multiplication factor  $\nu(T)$  is determined by the following integral equation (see eq. (4.1), p. 21, ref. [3])

$$\frac{du}{dT} (S_n(T) + S_e(T)) = \int_0^{T'_m} v(T') \sigma_{T'}^i(T, T') dT' \quad (5)$$

where  $T'_m$  is the maximum transferred energy to the struck nucleus and  $T'_m = T$  when  $M_1 = M_2$ , i.e., when the masses of the projectile and target atoms are equal.  $S_n$  and  $S_e$  are nuclear and electronic stopping cross sections, respectively. Stopping cross section is a measure of energy loss in the material. It is directly proportional to the stopping power,  $-dT/dx$ , energy loss per unit travelled path length, i.e.,  $-dT/dx = N S(T)$ , where  $N$  is the number of atoms per unit volume.

By previously mentioned assumptions, electrons do not contribute to displacement production. However, if electron energies are sufficiently high (above 1 MeV), it is observed in electron microscopy experiments that electrons do produce displacements [30]. In such a case, the contribution of electrons to the multiplication factor should be introduced into equation (5) as an extra term.

It is convenient to introduce the concept of damage energy,  $T_{dam}$ . The damage energy is the energy specifically transferred to target nuclei and therefore available to produce displacements. It can be determined by an equation similar to equation (5)

$$\frac{dT_{\text{dam}}}{dT} (S_n(T) + S_e(T)) = \int_0^{T_m} T_{\text{dam}}(T') \sigma_{T'}'(T, T') dT' \quad (6)$$

Lindhard et al. evaluated  $\sigma_{T'}'$  for screened Coulomb fields by the inverse power scattering law. They expressed many physical quantities in terms of dimensionless parameters. First, it is convenient to define a parameter  $T_L$ , which is given by

$$T_L = \frac{Z_1 Z_2 e^2}{a_L} \quad (7)$$

where  $a_L$  is the LSS screening radius given by

$$a_L = \beta a_0 [(Z_1)^{2/3} + (Z_2)^{2/3}]^{-1/2} \quad (8)$$

where  $a_0$  is the Bohr radius of hydrogen ( $0.529 \times 10^{-8}$  cm) and the coefficient  $\beta$ , which comes from the original Thomas-Fermi analysis, has the value  $(9\pi^2/128)^{1/3} = 0.8853$ . Then, the reduced parameters are

$$\text{reduced incident particle energy} = \epsilon = \frac{M_2 T}{M_1 + M_2 T_L} \quad (9)$$

$$\text{reduced transferred energy} = t = \frac{T T' M_2}{(2T_L)^2 M_1} \quad (10)$$

$$\text{reduced differential scattering cross section} = \sigma'_t = \frac{\pi(a_L)^2}{2t^{3/2}} f(t^{1/2}) \quad (11)$$

The scaling function  $f(t^{1/2})$  was numerically approximated by Winterbon et al. [31]. This approximation is given by

$$f(t^{1/2}) = \lambda t^{1/6} [1 + (2\lambda t^{2/3})^{2/3}]^{-3/2} \quad (12)$$

with  $\lambda = 1.309$ .

Finally, Lindhard and coworkers determined the asymptotic solution of equation (6) for the case  $Z_1 = Z_2$ . It is given by [3]

$$T_{\text{dam}}(T) = \frac{T}{1 + k_L g(\varepsilon)} \quad (13)$$

where the proportionality constant  $k_L$  is

$$k_L = (32/3\pi) (m/m_p)^{1/2} \frac{(Z_1)^{2/3} (Z_2)^{1/2} (A_1+A_2)^{3/2}}{Z^{1/2} (A_1A_2)^{1/2} A_1} \quad (14)$$

where  $Z_1$  and  $Z_2$  are the charge numbers for the projectile and target particles,  $A_1$  and  $A_2$  are the mass numbers for the projectile and target particles,  $m_p$  and  $m$  are the proton and electron masses, respectively, and  $(32/3\pi)(m/m_p)^{1/2}=0.0793$ .

$Z$  is given by

$$Z = [(Z_1)^{2/3} + (Z_2)^{2/3}]^{3/2} \quad (15)$$

The function  $g(\varepsilon)$  is graphically presented by Lindhard et al. [3]. The numerical approximation for this function is given by Robinson [32] as

$$g(\varepsilon) = 3.4008 \varepsilon^{1/6} + 0.40244 \varepsilon^{3/4} + \varepsilon \quad (16)$$

Lindhard's  $g(\varepsilon)$  function and Robinson's numerical approximation for this function, equation (16), are shown in figure 1.

The damage efficiency is defined as the fraction of the PKA energy which is available for the displacement production, and it is simply the ratio of the damage energy to the PKA energy,  $T_{\text{dam}}/T$ . Figure 2 shows the damage efficiencies as a function of the PKA energy for several elements according to LSS theory. The dashed line represents the ionization cutoff energy,  $T_I$ , given in

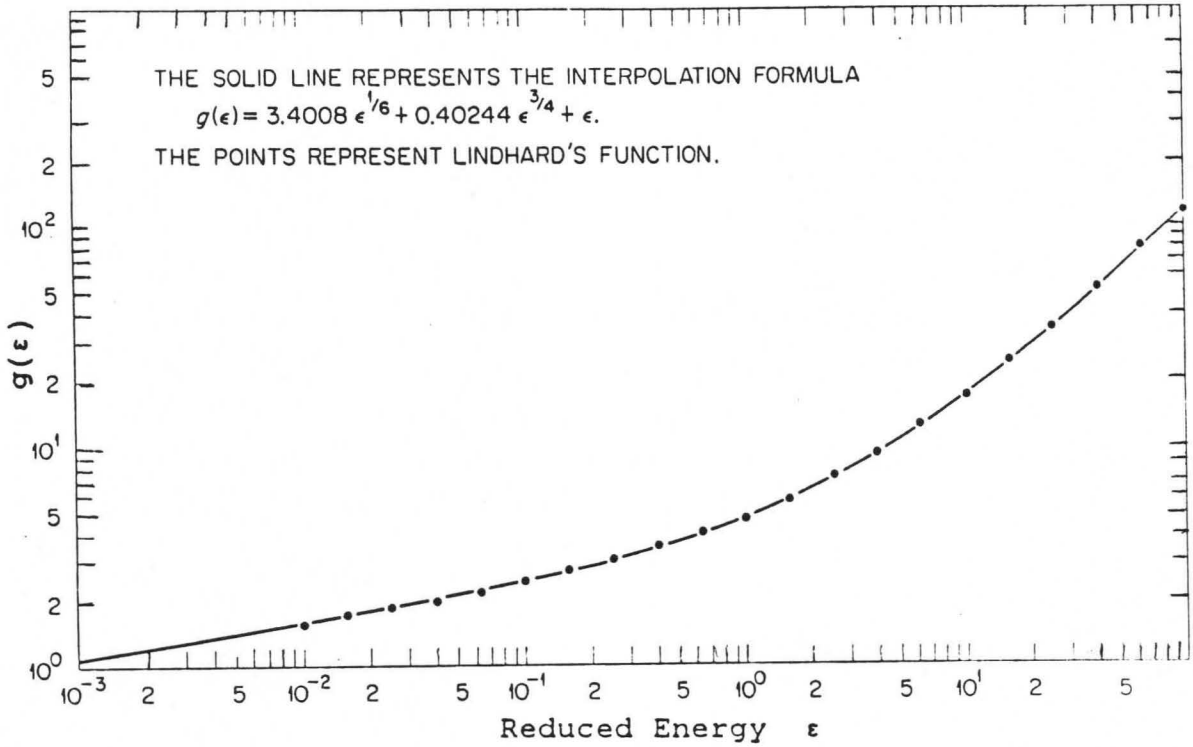


FIGURE 1. The  $g(\epsilon)$  function of Lindhard and the numerical approximation by Robinson [32]

equation (3). According to the Kinchin-Pease model modified with ionization corrections, given by equation (3), the damage efficiency is considered to be unity for energies below this cutoff energy. However, it is clearly seen that disregarding the ionization losses is a poor approximation even at very low PKA energies.

Lindhard's asymptotic solution (13) is valid for monoatomic systems ( $Z_1=Z_2$ ). There is also a limitation regarding the energy of the incident particle. It must be lower than  $0.0248 M_1 Z_1^{4/3}$  (MeV), where  $M_1$  is the mass of



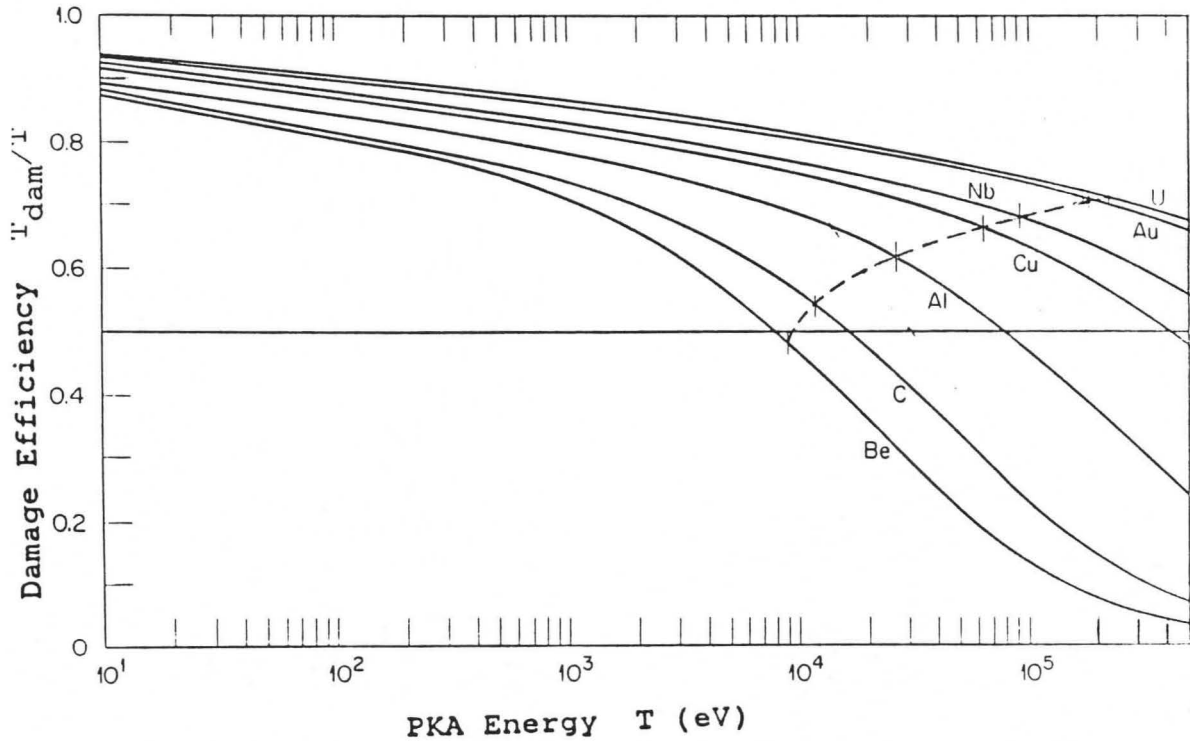


FIGURE 2. Damage efficiencies as a function of PKA energy according to LSS theory (Dashed line represents the ionization cutoff energies [32])

the projectile in amu. This limitation comes from the electronic stopping cross section, which is a part of the theory. The first limitation, i.e.,  $Z_1=Z_2$ , however, may be relaxed if the ratio of the atomic numbers of incident and target atoms does not differ too much from unity. Neutron-damage calculations for light elements, such as beryllium and carbon, in a fission or fusion neutron spectrum by LSS theory are of limited reliability [33]. It should be noted that the LSS theory gives only the average concentration of displacements with no information concerning their

distribution in the irradiated material.

A standard procedure to calculate the number of displacements is suggested by Robinson and Oen [12] and Norgett et al. [13]. Their suggestions are:

1. The coefficient  $\kappa$  in (4) may be taken to be 0.8, as an approximation to Sigmund's value of 0.84, as given in equation (4).  $\kappa$  is independent of PKA energy.
2. Damage energy,  $T_{\text{dam}}$ , should be calculated according to the LSS model, in order to take ionization losses into account.

Then,  $v(T)$  becomes

$$v(T) = \begin{cases} 0 & , T < T_d \\ 1 & , T_d \leq T < 2T_d \\ \kappa T_{\text{dam}}/(2T_d) & , 2T_d \leq T \end{cases} \quad (17)$$

The effects of different kinds of irradiation can be compared by means of several parameters. Displacement cross section  $\sigma_d$  can be considered as the first parameter. It may be interpreted as the displacement rate per atom of material per unit flux of incident particles. It is given by

$$\sigma_d(E) = \int_{T_d}^{T_m} \sigma_T'(E, T) v(T) dT \quad (18)$$

where  $\sigma_T'$  is the differential scattering cross section with respect to transferred energy  $T$  and  $T_m$  is the maximum transferred energy. The lower limit of the integral may be taken as zero if incident particle energy is higher than several keV [14]. Another similar parameter is damage energy cross section  $\sigma_{de}$ . By the same fashion, it is written as

$$\sigma_{de}(E) = \int_{T_d}^{T_m} \sigma_T'(E, T) T_{dam}(T) dT \quad (19)$$

The displacement production rate  $K_d$  gives the number of displacements produced per atom per unit time. It is given by

$$K_d = \int_0^{\infty} \phi_E'(E) \sigma_d(E) dE \quad (20)$$

where  $\phi_E' dE$  is the number of incident particles with energies between  $E$  and  $E+dE$  crossing unit area per unit time. For monoenergetic radiations,  $K_d$  is simply given by

$$K_d = \phi \sigma_d \quad (21)$$

Similarly, the amount of energy transferred to target nuclei per atom per unit time is

$$K_{de} = \int_0^{\infty} \phi'_E(E) \sigma_{de}(E) dE \quad (22)$$

For several reasons, the basic theory predicts different defect densities and distributions compared to the experimental observations. One of the reasons is dynamic and thermal annealing [34]. The sum of the formation energies for an isolated vacancy-interstitial pair is about 5 eV, whereas the displacement threshold energy is of order of 20 to 50 eV for many metals [14]. Therefore, a considerable proportion of energy spent in the production of displacements is dissipated by thermal vibrations. Thus, mechanically unstable close vacancy-interstitial pairs may recombine athermally. Furthermore, interstitials may become mobile at a temperature as low as 30 K for many metals. Therefore, thermally activated motion of defects results in annihilation through recombination. Inelastic energy losses also play an important role. In general, the theory predicts the energy loss of a moving particle by a number of random two body collisions without any account taken of the

crystalline structure of the irradiated material. However, it has been observed by experiments and computer simulations [35,36] that energetic particles have higher penetration distance in crystalline material as compared to the amorphous form of the same material. In crystalline material, a particle may move in open channels between regularly arranged atom rows, where it loses its energy by many glancing collisions, which yield low energy transfers. This phenomenon is known as channeling. Thus, the number of defects produced in such a crystalline material is lower than that predicted by the basic theory. The effect of the crystalline structure is more pronounced for incident ions directed along low index directions, and is not very significant for a single random cascade development [37]. Inaccuracy in the scattering parameters is another source for discrepancy. In some cases, these parameters are 100% in error especially in the low energy region [38]. A better agreement between theoretical predictions and experimental observations can be achieved by consideration given to these factors.

## STOPPING OF ENERGETIC IONS IN MATTER

The energy loss process of ions is important for understanding of the interaction of charged particles with matter. In general, energetic particles may lose their energy by energy transfer to nuclei (displacement production), energy transfer to electrons (ionization), photon emission, and nuclear reactions. In the case of neutrons, energy losses due to these processes may be appreciable at energies as low as a few eV because of high reaction cross sections. However, energy loss of charged particles via photon emission and nuclear reactions is not significant in the traditional energy range of interest in radiation damage studies (up to few MeV). Slowing of charged particles, especially heavy ions, by transferring their energies to struck nuclei is most effective at low velocities. Energy transferred to electrons becomes dominant at high velocities. However, energy loss by transferring energy to nuclei and electrons should be considered as a continuous process. Bohr [6] suggested that the energy loss of ions could be separated into two components; nuclear and electronic energy losses.

In the stopping of energetic ions, the differential scattering cross section,  $\sigma_T^I$ , for transferring energy within unit energy range at  $T'$  is of interest. Stopping power,  $-(dT/dx)$ , is a measure of the energy loss of

energetic particles. Stopping power is defined as the energy loss of moving particle per unit length traveled within the target, and given as

$$\frac{dT}{dx} = - N \int_0^{T_m} T' \sigma_{T'}^i(T, T') dT' \quad (23)$$

where  $N$  is the number of target atoms per unit volume. The integral on the right hand side is the stopping cross section. Stopping cross section can be divided into two parts, nuclear and electronic. Then, total energy loss per unit path length can be represented by

$$\frac{dT}{dx} = - N (S_n(T) + S_e(T)) \quad (24)$$

$S_n$  and  $S_e$  are stopping cross sections for energy loss to the target nuclei and electrons, respectively. Although the nuclear stopping is more important from the radiation damage point of view, both nuclear and ionization energy losses should be examined.

## Nuclear Stopping

Energy loss to target nuclei can be represented by purely elastic collisions. The simplest case of scattering can be represented as a two-body collision. Consider a target atom of charge number  $Z_2$  and mass  $M_2$  to be initially at rest in the laboratory system. Let the projectile particle, assumed to be a PKA with  $Z_1$  and  $M_1$ , have an energy  $T$  before the collision with the target atom. After the collision, the target nucleus possesses energy  $T'$  while the energy of the projectile is reduced to  $(T-T')$ . Since we consider only elastic collisions here,  $Q$ ,  $U$ , and  $U_i$  (discussed on page 14) are neglected. Classical mechanical treatment gives the scattering angle  $\theta$  in the center-of-mass system (CMS) as [39,40]

$$\theta = \pi - 2p \int_p^\infty \frac{dr}{r^2 f(r)} \quad (25)$$

where

$$f(r) = \left( 1 - \frac{V(r)}{T_{cm}} - \frac{p^2}{r^2} \right)^{1/2} \quad (26)$$

and



$r$  = separation distance between particles,

$p$  = impact parameter, the distance between the initial directions of motion of incident and struck particle,

$\rho$  = the distance of closest approach, which corresponds to  $r$  when  $f(r)$  is equal to zero,

$V(r)$  = potential energy of particles,

$T_{\text{cm}}$  = the total kinetic energy of the particles in the CMS.

$T_{\text{cm}}$  is given by

$$T_{\text{cm}} = \frac{M_2}{M_1 + M_2} T \quad (27)$$

The energy  $T'$  is related to the scattering angle  $\theta$  in the CMS by

$$T' = \frac{4 M_1 M_2}{(M_1 + M_2)^2} T \sin^2 (\theta/2) \quad (28)$$

In case of a head-on collision  $\theta$  corresponds to  $\pi$ , and  $T'$  becomes maximum transferred energy  $T'_m$

$$T'_m = \frac{4 M_1 M_2}{(M_1 + M_2)^2} T \quad (29)$$

The scattering cross section is expressed in terms of the impact parameter by

$$d\sigma = 2 \pi p dp \quad (30)$$

Once the potential  $V(r)$  is known, the impact parameter can be expressed in terms of the scattering angle by means of (25) and (26). Then, the relation between  $T'$  and  $\theta$  can be found by (28). Thus, the differential scattering (or, here, energy transfer) cross section is determined for a specified potential. Equation (25) can be solved analytically if the potential function has a simple form such as the Coulomb potential,

$$V(r) = \frac{Z_1 Z_2 e^2}{r} \quad (31)$$

which represents Rutherford scattering. For the Coulomb potential, the differential scattering cross section is

$$\sigma_{T'}^1 = \pi (\rho_0/2)^2 T'_m (T')^{-2} \quad (32)$$

where  $\rho_0$  is the collision diameter given by

$$\rho_0 = \frac{M_1 + M_2}{M_2} \frac{Z_1 Z_2 e^2}{T} \quad (33)$$

The collision diameter is the distance of closest approach in a head-on collision ( $p = 0$ ) for a Coulomb potential. The Rutherford scattering is valid for close collisions, i.e., small  $\rho$  values. For larger  $\rho$ 's, the Coulomb potential must be considered to be screened by the orbital electrons.

Deviations from Rutherford scattering are observed when the velocity of the projectile becomes comparable to the orbital velocities of electrons, i.e., at relatively low velocities. The orbital velocities of the most loosely bound (outermost) orbital electrons,  $v_1$ , can be estimated by [18]

$$v_1 = (Z_1)^{2/3} v_0 \quad (34)$$

where  $v_0$ , the Bohr velocity, is  $e^2/\hbar$ , where  $\hbar$  is  $h/2\pi$  and  $h$  is Planck's constant.

The interaction potential for screened Coulomb fields can be written as

$$V(r) = \frac{Z_1 Z_2 e^2}{r} \phi(r/a) \quad (35)$$

where  $\phi(r/a)$  is the screening function and  $a$  is the screening length. Bohr's suggestion for  $\phi(r/a)$  was [6]

$$\phi(r/a) = \exp(-r/a_B) \quad (36)$$

with screening length

$$a_B = a_o ((Z_1)^{2/3} + (Z_2)^{2/3})^{-1/2} \quad (37)$$

Despite the simplicity of the screening function in (36), Lindhard et al. sought another form for a more accurate description of the interaction [5]. Their choice for this function is

$$\phi(r/a) = (k_s/s) (a_L/r)^{s-1} \quad (38)$$

where, as in (8)

$$a_L = \beta a_o ((Z_1)^{2/3} + (Z_2)^{2/3})^{-1/2} \quad (39)$$

and  $k_s$  is a constant and variable  $s$  depends on the minimum separation distance  $\rho$ . For small  $\rho$ , i.e., for Coulomb interactions,  $s$  is equal to 1 and it increases with increasing  $\rho$ . Lindhard et al. approximate  $\phi(r/a)$  for overall  $s$  values by [5]

$$\phi(r/a) = 1 - r (r^2 + 3(a_L)^2)^{-1/2} \quad (40)$$

LSS finds the scattering angle (assuming that it is small) to be

$$\theta = \gamma_s a_L \rho^{-2} k_s \quad (41)$$

where  $\gamma_s$  is expressed in terms of the beta function  $B$  such

that

$$\gamma_s = - \frac{1}{2} B\left[-\frac{1}{2}, \frac{s+1}{2}\right] = - \left(\frac{1}{s}\right)^{1/2} \quad (42)$$

where the beta function is given by [41]

$$B[z, w] = 2 \int_0^{\pi/2} (\sin \tau)^{2z-1} (\cos \tau)^{2w-1} d\tau \quad (43)$$

The differential scattering cross section for this potential is given by

$$\sigma_{T'}^i = (\pi/s) [(\rho_0/2)(a_L)^{s-1} k_s \gamma_s]^{2/s} \frac{(T_m')^{1/s}}{(T')^{1+1/s}} \quad (44)$$

For practical purposes,  $\sigma_{T'}^i$  is expressed in terms of reduced parameters. This form of the scattering cross section is given by equation (11). The scaling function,  $f(t^{1/2})$ , gives overall fit so that the  $s$  dependency of the scattering cross section is avoided. The values of  $f(t^{1/2})$  were tabulated by Lindhard et al. for  $t^{1/2}$  values in the range of 0.002 to 40. For very small values of  $t$ ,  $t^{1/2} < 0.002$ ,  $f(t^{1/2})$  behaves as  $1.43x(t^{1/2})^{0.35}$ .  $f(t^{1/2})$  for

large  $t^{1/2}$  (the Rutherford scattering) is  $(2 t^{1/2})^{-1}$  [5].

Reduced nuclear stopping cross section,  $s_n$ , is another dimensionless parameter. It can be obtained by means of the scaling function  $f(t^{1/2})$  such that

$$s_n(\varepsilon) = - \frac{1}{\varepsilon} \int_0^{\varepsilon} f(t^{1/2}) d(t^{1/2}) \quad (45)$$

The values of  $s_n$  are also tabulated by Lindhard et al. [5] for  $\varepsilon$  values between 0.002 and 40. If  $\varepsilon$  is greater than 10, the limiting function for  $s_n$  is

$$s_n(\varepsilon) = \frac{\ln(1.294 \varepsilon)}{2 \varepsilon} \quad (46)$$

For small values of  $\varepsilon$ ,  $s_n$  can be approximated by

$$s_n(\varepsilon) = 1.059 \varepsilon^{0.35} \quad (47)$$

$s_n(\varepsilon)$  is directly proportional to  $S_n(T)$ . The relation between these two nuclear stopping cross sections is

$$S_n(T) = 4 \pi (a_L)^2 \frac{M_1}{M_1+M_2} T_L s_n(\varepsilon) \quad (48)$$

The reduced nuclear stopping cross section  $s_n(\varepsilon)$  for the Bohr potential, equations (35) and (36), is given by [38]

$$s_n(\varepsilon) = \frac{A \ln(B\varepsilon)}{B\varepsilon - (B\varepsilon)^{-C}} \quad (49)$$

where the fitted constants A, B, and C are given as 0.51661, 1.4821, and 0.83273, respectively.

Another form of screened Coulomb potential was suggested by Molière. The screening function for this potential is [39]

$$\phi(r/a) = \sum_{i=1}^3 C_i \exp(-b_i r/a_M) \quad (50)$$

where

$$a_M = \beta a_0 ((Z_1)^{1/2} + (Z_2)^{1/2})^{-2/3} \quad (51)$$

where  $\beta$  is given in (8) and the other constants are

$$\begin{aligned} C_1 &= 0.35 & b_1 &= 0.30 \\ C_2 &= 0.55 & b_2 &= 1.20 \end{aligned}$$

$$C_3 = 0.10 \quad b_3 = 6.00$$

The reduced nuclear stopping cross section for the Molière potential is given by [38]

$$s_n(\varepsilon) = \frac{0.5 \ln(1+\varepsilon)}{\varepsilon + A \varepsilon^B} \quad (52)$$

where constants A and B are 0.051953 and 0.32011, respectively.

In general, all screened Coulomb potentials approach the same  $s_n(\varepsilon)$  values for large  $\varepsilon$  values. This corresponds to the stopping cross section of the unscreened Coulomb potential. However, each screened Coulomb potential shows its own characteristics at small values of  $\varepsilon$  as shown in figure 3.

According to Wilson et al. [38], low energy stopping powers based on statistically derived potentials, such as the Thomas-Fermi potential, give underestimated results. For  $\varepsilon$  values between 0.03 and 0.3, experimentally deduced nuclear stopping powers are 30% higher than theoretical predictions. These deviations increase (over 100%) for  $\varepsilon$  smaller than 0.0006. Wilson et al. represented their experimentally observed potential by a semiempirical relation similar to the Molière potential. The screening



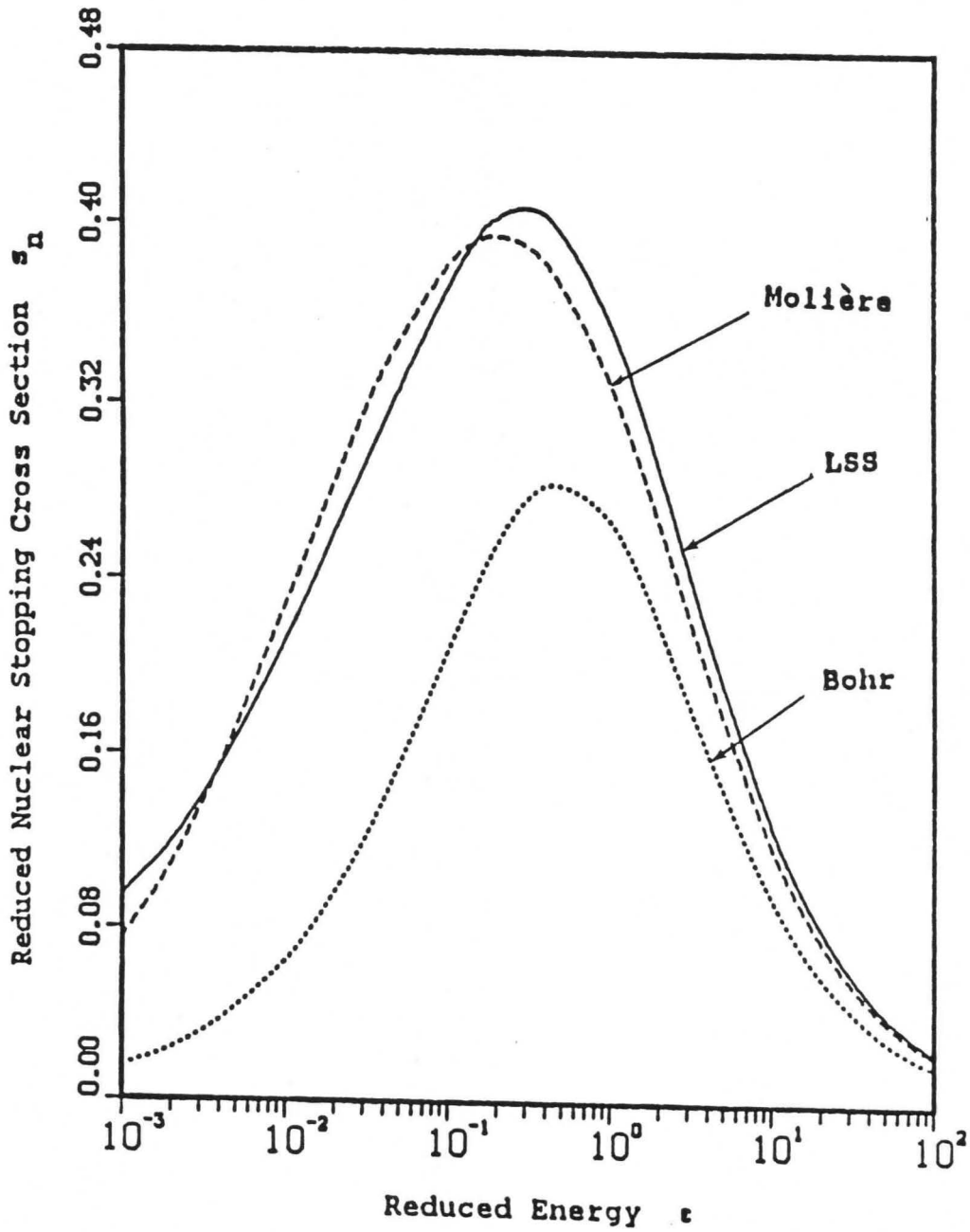


FIGURE 3. The reduced nuclear stopping cross sections for Bohr, Molière, and LSS potentials

function of this potential is in the form of equation (49).

Corresponding constants are [38]

$$c_1 = 0.06905 \quad b_1 = 0.131825$$

$$c_2 = 0.166929 \quad b_2 = 0.307856$$

$$c_3 = 0.826165 \quad b_3 = 0.916760$$

and the screening length is given by equation (51). As it is shown in figure 4 for a Cu-Cu interaction, the Bohr potential is too heavily screened and the LSS potential is too weakly screened compared to the experimentally derived Wilson potential. However, Molière approximation gives a better agreement especially at large separation distances.

#### Electronic Stopping

Although the energy transfer to nuclei is important for radiation damage studies, the energy transfer to electrons (ionization loss) is the principal energy loss mechanism over a wide energy range. Nuclear energy losses are dominant over ionization losses only at low energies. However, ionization losses should not be neglected even at very low energies.

An ion moving at a velocity higher than the velocities of its electrons loses energy primarily by collisions with target electrons. The electrons of a projectile are stripped off the atom if they are slower than the projectile

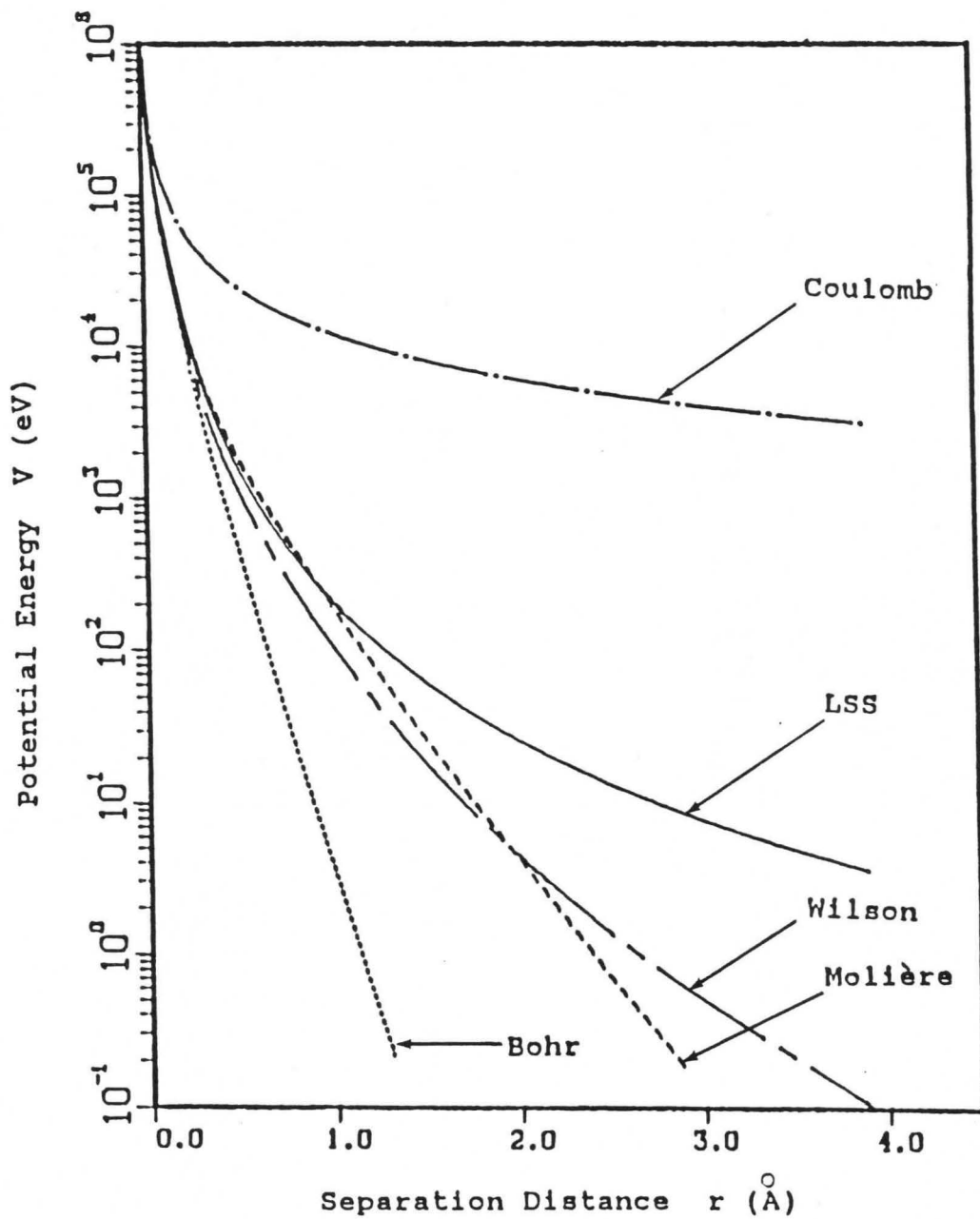


FIGURE 4. Variation of potential with separation distance for a Cu-Cu interaction according to Coulomb, Bohr, LSS, Molière, and semiempirical Wilson potentials

itself. As the projectile particle slows down, the projectile velocity becomes lower than the velocity of its electrons. At lower velocities, energy transfer to target nuclei starts being more effective.

The electronic energy loss of a moving ion is closely related to its velocity and charge. For heavy ions, nuclear and effective charges may be distinguished. Nuclear charge,  $Z_1$  for the projectile, is directly proportional to the total number of electrons. On the other hand, effective charge,  $(Z_1)^*$ , is the number of electrons remaining, when some electrons have been stripped from the moving ion. The average charge state of an ion can be predicted by estimating the number of electrons whose velocities are lower than the velocity of the ion.

The Thomas-Fermi atom model estimates the effective charge of an ion as [18]

$$(Z_1)^* = (Z_1)^{1/3} (v/v_0) \quad (53)$$

where  $v_0$  is the Bohr orbital velocity, given by  $e^2/\hbar$  ( $=2.188 \times 10^8$  cm/sec). Theoretical treatments of electronic energy losses based on the Thomas-Fermi model were developed by Lindhard et al. [4,5] and Firsov [7,8]. Both theories estimate the average electronic stopping power at low energies to be proportional to the velocity.

The Lindhard-Scharff-Schiott (LSS) electronic stopping cross section is represented by the well-known formula [4]

$$S_{e,L}(T) = - \frac{1}{N} \frac{dT}{dx} \Big|_e = \xi \frac{8 \pi e^2 a_0 Z_1 Z_2}{Z} \frac{v}{v_0} \quad (54)$$

where  $T$  and  $v$  are the energy and velocity of the moving projectile ion,  $x$  is the distance along its path, and  $Z_1$  is its nuclear charge.  $Z_2$  is the nuclear charge for the target ion, and as in (15)

$$Z = ((Z_1)^{2/3} + (Z_2)^{2/3})^{3/2} \quad (55)$$

Also,  $a_0 = \hbar^2/me^2$  is the Bohr radius ( $e$ = electron charge, and  $\hbar=h/2\pi$ , where  $h$ = Planck's constant).  $\xi$  is a proportionality constant in the range of 1 to 2. The best value for  $\xi$  is approximated by  $\xi=(Z_1)^{1/6}$ . According to the LSS model, equation (54) is valid as long as the projectile velocity is lower than the velocities of electrons. The velocity of electrons is approximated by  $v_1=v_0 (Z_1)^{2/3}$ , as in (34).

LSS expressed their electronic stopping cross section (equation (54)) in terms of dimensionless quantities, as follows

$$s_e(\varepsilon) = (d\varepsilon/d\rho_L)_e = k_L \varepsilon^{1/2} \quad (56)$$

where

$$\epsilon = \text{reduced energy} = \frac{M_2}{M_1+M_2} \frac{T}{T_L} \quad (57)$$

$$\rho_L = \text{reduced path length} = N 4 \pi (a_L)^2 \frac{M_1 M_2}{(M_1+M_2)^2} R \quad (58)$$

and

$$k_L = \frac{32}{3\pi} \frac{(Z_1)^{2/3} (Z_2)^{1/2}}{Z^{1/2}} \left( \frac{M_1+M_2}{M_1} \right)^{3/2} \left( \frac{m}{M_2} \right)^{1/2} \quad (59)$$

In the above equations,  $m$ ,  $M_1$ , and  $M_2$  are the electron, projectile, and target masses, respectively,  $N$  is the number of atoms per unit volume, and  $a$  is the screening length, given by (as in (39))

$$a_L = \beta Z^{-1/3} a_0 \quad (60)$$

where  $Z$  is given by (55). When the projectile and target particles are the same, and

$$Z_1 = Z_2 = Z_c$$

$A$  = mass number of the projectile and target particles,

$m$  = electron mass in atomic mass units (amu),

then it may be shown that

$$k_L = (32m/\pi) 2^{3/4} (Z_c)^{2/3} A^{-1/2} = 0.133 (Z_c)^{2/3} A^{-1/2} \quad (61)$$

In the Firsov theory, electronic energy losses are related to the impact parameter. This theory has been widely used for the treatment of the inelastic energy loss of ions in crystalline material [26]. Firsov used the Thomas-Fermi model for electron distributions of two colliding atoms to obtain numerical results. This analysis resulted in the following formula for the ionization losses,  $Q$ , in a single collision in terms of the distance of the closest approach,  $\rho$ , [8]

$$Q = \frac{0.35 (Z_1 + Z_2)^{5/3} \hbar v / a_0}{[1 + 0.16 (Z_1 + Z_2)^{1/3} \rho / a_0]^5} \quad (62)$$

The stopping cross section associated with equation (62) is given by [42]

$$S_{e,F} = 7.51 (3 \pi^2 \hbar a_0 / 32) (Z_1 + Z_2) v \quad (63)$$

The applicable velocity range for equation (63) is the same as that for equation (54).

Lindhard and Firsov theories have been widely used to analyze the behavior of low energy charged particles. The

two theories generally agree with experimental observations from the point of view of the use of a velocity-proportional stopping power in the low energy region. However, some deviations from the proportionality are observed when the projectile velocity is close to the velocity of its electrons. For this reason, the upper velocity limit for the applicability of both theories may be taken to be much lower than  $v_1 (= v_0(Z_1)^{2/3}$ , where  $v_0 = e^2/\hbar$ ).

Fastrup et al. [17] analyzed the effect of projectile's charge on the electronic stopping cross section of carbon. They used a number of projectiles having charge numbers between 6 and 20 with a constant incident velocity. When the electronic stopping cross section is displayed as a function of the projectile charge number,  $Z_1$ , at a constant velocity, the LSS and Firsov theories predict an increasing cross section as  $Z_1$  increases. However, experimental results showed some oscillations in stopping cross section [18], known as  $Z_1$  oscillations. The relative amplitudes of these oscillations were observed to decrease with increasing incident velocity. Later, similar oscillations were observed when the stopping powers of several target materials for a specified projectile were displayed as a function of the charge number of target atoms,  $Z_2$ , again at a constant projectile velocity. These are known as  $Z_2$  oscillations [18].



An alternative method to determine the electronic stopping cross section of heavy ions is the use of the effective charge concept. This concept states that the ratio of stopping cross sections of any target and for two different projectiles (A and B) is equal to the square of the ratio of these projectiles' effective charges if both projectiles have the same velocity, i.e.,

$$\frac{S_e(Z_{1,A}, Z_2, v)}{S_e(Z_{1,B}, Z_2, v)} = \left[ \frac{(Z_{1,A}, v)^*}{(Z_{1,B}, v)^*} \right]^2 \quad (64)$$

In practice, the cross sections for heavy projectiles are often determined by calculation from the measured cross section for protons, since there are ample data for proton stopping and the highest accuracy in the prediction of electronic stopping cross section is achieved for protons. Furthermore, experimental studies show that the effective charge of protons can be considered to be unity [10]. Thus, equation (64) is reduced to

$$S_e(Z_1, Z_2, v) = [(Z_1)^*]^2 S_{e,p}(Z_2, v) \quad (65)$$

where  $S_{e,p}$  is the electronic stopping cross section for protons.

The effective charge of moving ion  $(Z_1)^*$  is generally determined based on the experimental results. Semiempirical

expressions for  $(Z_1)^*$  have been generally expressed in the following form [18]

$$(Z_1)^* = Z_1 \left[ 1 - C \exp\left(-\frac{\alpha v}{v_0 (Z_1)^\gamma}\right) \right] \quad (66)$$

where  $C$ ,  $\alpha$ , and  $\gamma$  are adjustable parameters.  $\gamma$  has been generally chosen as  $2/3$  due to a Thomas-Fermi argument [18]. After the compilation of a large number of experimental data, Brown and Moak suggested the following semiempirical relation for heavy ions [22]

$$(Z_1)^* = Z_1 \left[ 1.034 - \exp\left(-\frac{v}{v_0 (Z_1)^{0.688}}\right) \right] \quad (67)$$

Most of the semiempirical relations for  $(Z_1)^*$  have been proposed as a function of velocity relative to the Bohr velocity  $v_0$ . Recently, Kreussler and collaborators suggested that the effective charge should depend on, not only the projectile velocity, but also the velocity of the conduction electrons of the medium. In other words, effective charge is a function of the relative velocity between projectile and the conduction electrons of the medium,  $v_e$  [43].

$v_e$  was determined in terms of the Fermi velocity of solid [43]

$$v_e = (3/5)^{1/2} v_F \quad (68)$$

Then, Fermi velocity was expressed as a function of the electron radius,  $r_s$ , as

$$v_F = 1.919/r_s \quad (69)$$

All physical quantities were expressed in atomic units, i.e., relative to  $e$ ,  $\hbar$ ,  $m$ , or  $v_0$ .

In Brandt's theory, the ionization fraction,  $q$ , of a moving ion is given by [9]

$$q = \frac{Z_1 - n}{Z_1} \quad (70)$$

where  $n$  is the number of electrons still bound to the projectile at relative velocity  $v_r$ . The relative velocity of the ion is defined as [44]

$$v_r(v, v_F) = \begin{cases} v_F (15 + 10\alpha^2 - \alpha^4)/20 & , v \leq v_F \\ v (5 + \alpha^2)/5 & , v \geq v_F \end{cases} \quad (71)$$

where  $\alpha = (v/v_F)$ .

Brandt et al. proposed that the ionization fraction  $q$  is the same for all ions as long as they have the same reduced velocity  $y_r$ , where

$$y_r = (v_r/v_o) (Z_1)^{-2/3} \quad (72)$$

However, the screening of the ion by the electrons will be different for each ion, i.e., screening is a function of the charge number of the projectile. Brandt et al. expressed the screening length  $\Lambda$  by [9]

$$\Lambda = \frac{0.48 (1-q)^{2/3}}{(Z_1)^{1/3} [1-(1-q)/7]} \quad (73)$$

In distant collisions, i.e., impact parameter  $p > \Lambda$ , electrons in the medium interact with the moving ions as if they were point charges with  $Q_i = q Z_1$ .  $Q_i$  is the ionic charge number of the projectile. On the other hand, at smaller impact parameters,  $p < \Lambda$ , the electrons of the medium can penetrate into the electron cloud and undergo close collisions. In such a case, the effective charge of the ion is greater than the ionic charge. In other words, the effective charge fraction  $\zeta (= (Z_1)^*/Z_1)$  is greater than  $q$  [10].

The effective charge fraction is expressed in terms of  $q$ ,  $\Lambda$ , and the Fermi momentum  $p_F$ .  $p_F$  has the same magnitude as the Fermi velocity  $v_F$  in atomic units. For the small

values of  $(2p_F\Lambda)$ ,  $\zeta$  is given by [44]

$$\zeta = q + C(p_F) (1-q) \ln (1 + (2 p_F \Lambda)^2) \quad (74)$$

where  $C(p_F)$  is a material-dependent constant equal to approximately 0.5. Then, the stopping cross section for heavy ions is calculated by

$$S_{e,B}(v) = \zeta^2 (Z_1)^2 S_{e,p}(v) \quad (75)$$

Mann and Brandt [44] analyzed the existing low energy stopping theories for protons. They found that a recently developed theory, the scattering theory with self-consistent ion screening or the Echenique, Nieminen, and Ritchie (ENR) approximation gives the best agreement with experimental observations compared to the Lindhard-Winther dielectric approximation, The Fermi-Teller theory, and the linear response theory of Ritchie. Mann and Brandt write the stopping cross section in the form

$$S_{e,p} = \frac{1}{N} f(v_F) \frac{v}{v_F} \quad (76)$$

The analytic form of the scattering function  $f(v_F)$  for ENR model is approximated by means of the Lindhard-Winther scattering function  $f_{LW}$  in a limited range of  $r_s$  between 1.49 and 2.23 a. u. The approximation is [44]

$$f_{\text{ENR}}(v_F) = 1.63 f_{\text{LW}}(v_F) \quad (77)$$

The scattering function  $f_{\text{LW}}$  is given by

$$f_{\text{LW}}(v_F) = 2 \omega (v_F)^2 \{ \ln[(\omega+2)/3] - (\omega-1)/(\omega+2) \} / (\omega-1)^2 \quad (78)$$

where  $\omega = 3\pi v_F$ . The scattering function  $f$  can be converted from atomic units to conventional stopping power units (MeV/cm) by multiplication with  $(e/a_0)^2$ , i.e.,  $5.142 \times 10^3$  MeV/cm.

Brandt and coworkers deduced the ionization fraction,  $q$ , of ions in solids as a function of reduced velocity  $y_r$  based on various experimental observations [9]. In the calculation of  $q$  values, they used an adjustable parameter, the velocity stripping parameter,  $b$ . Their suggestions for  $b$  values are 1.26 for light ions and 1.33 for heavy ions. The ionization curve for  $b=1.33$  is shown in figure 5. If another  $b$  value is chosen at a given  $q$ , the reduced velocity can be adjusted to a new value,  $(y_r)'$ , such that

$$(y_r)' = (b/1.33) y_r \quad (79)$$

Ziegler et al. [45] analyzed Brandt's approach to the ionization. Using existing experimental stopping data for heavy ions and the same theoretical concepts, they reevaluated the ionization curve. According to their results, Brandt's curve is consistent with their curve for  $y_r$  values greater than about 0.7. On the other hand,  $q$

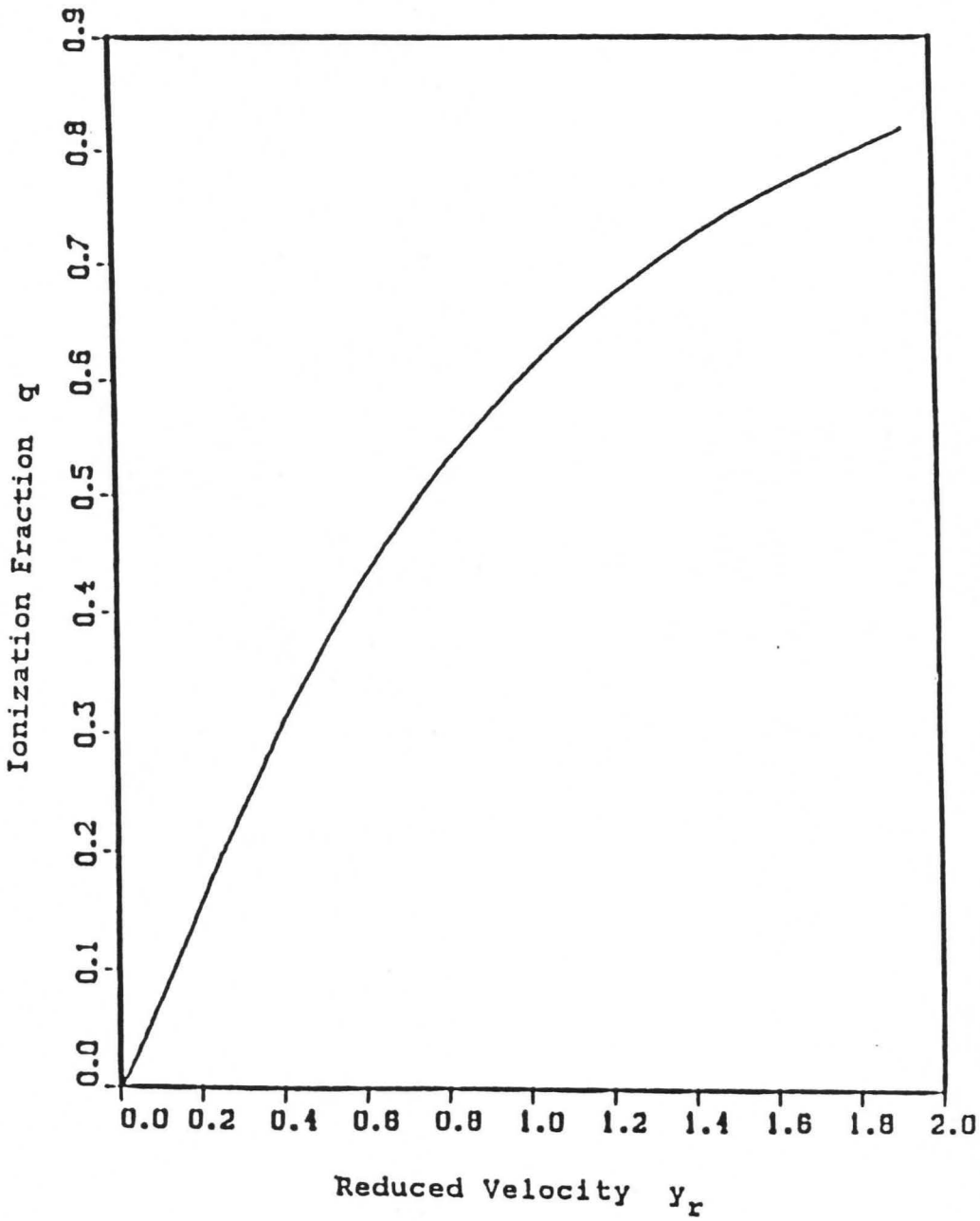


FIGURE 5. Ionization curve for heavy ions with velocity stripping parameter  $b=1.33$

values diverge below this  $y_r$  value. In this region, Ziegler et al. observed lower  $q$  values compared to Brandt's data.

Krist and Mertens compared the results of their effective charge measurements for light ions with the predictions of Brandt's theory [46]. Their ionization curve, which is evaluated based on Brandt's approach, lies above the curve given by Brandt and coworkers. According to their observations, experimental  $q$  values are 4-22% greater than the original  $q$  values and deviations increase with increasing  $y_r$ .

These discrepancies might have resulted from using different proton stopping data as well as employing different methods in the elimination of nuclear stopping power from total stopping power. Ziegler et al. suggest that the screening parameter  $\Lambda$  can be multiplied by a correction factor and used as an adjustable parameter [45].

Although electronic stopping power is fairly well approximated for energies greater than 1 MeV/amu, accuracy in the stopping power decreases with decreasing energy. Below this energy, theoretical stopping powers should be corrected according to experimental observations whenever possible.



## RESULTS: DAMAGE ENERGY CALCULATIONS

In order to determine the radiation damage produced by any kind of irradiation, it is necessary to know the partition of the transferred energy between target nuclei and electrons. Energy transferred to target nuclei, so-called damage energy  $T_{\text{dam}}$ , contributes to displacement production, whereas energy spent in the ionization of electrons dissipates as heat.

Damage energy for a single collision cascade initiated by a PKA of energy  $T$  for the case  $Z_1=Z_2$  was evaluated by Lindhard et al. [3] based on their theoretical approach. In general, damage energy for any target-projectile combination can be determined by (see, equation (6))

$$T_{\text{dam}}(T) = \int_0^T \frac{1}{S_n(T) + S_e(T)} \int_0^{T_m} T_{\text{dam}}(T') \sigma_{T'}^1(T, T') dT' dT \quad (80)$$

This equation can be used if the target is thick enough so that projectile particle is completely stopped within the target. If the projectile emerges from the target with any amount of energy, the previous equation should be replaced by [47]

$$T_{\text{dam}}(T) = N \int_0^x \int_0^{T_m'(T(x'))} T_{\text{dam}}(T') \sigma_{T'}^I(T, T') dT' dx' \quad (81)$$

where  $x$  is the range of moving particle in target and  $T(x')$  is the energy of projectile at any point  $x'$  along the path.

The solution of the integral equation (80) was evaluated by Lindhard et al. [3] to be

$$T_{\text{dam}}(T) = \frac{T}{1+k_L g(\varepsilon)} \quad (82)$$

where  $\varepsilon = (T/T_L) M_2/(M_1+M_2)$  as in (9) and  $g(\varepsilon)$  is given by (16). The proportionality constant  $k_L$  for the LSS electronic stopping power is given by equation (14).

$T_{\text{dam}}(T)$  was determined in the present work for the Firsov theory as follows. It was assumed that for the Firsov theory  $T_{\text{dam}}(T)$  takes the same form as in (82), except for a difference in the  $k$  factor that multiplies  $g(\varepsilon)$ . In particular, we have let

$$k_F = k_L (S_{e,F}/S_{e,L}) \quad (83)$$

where  $S_{e,F}$  and  $S_{e,L}$  are the Firsov and Lindhard electronic stopping cross sections. Figure 6 shows that for both theories the stopping cross power is proportional to velocity, as is also seen in equations (54) and (63).

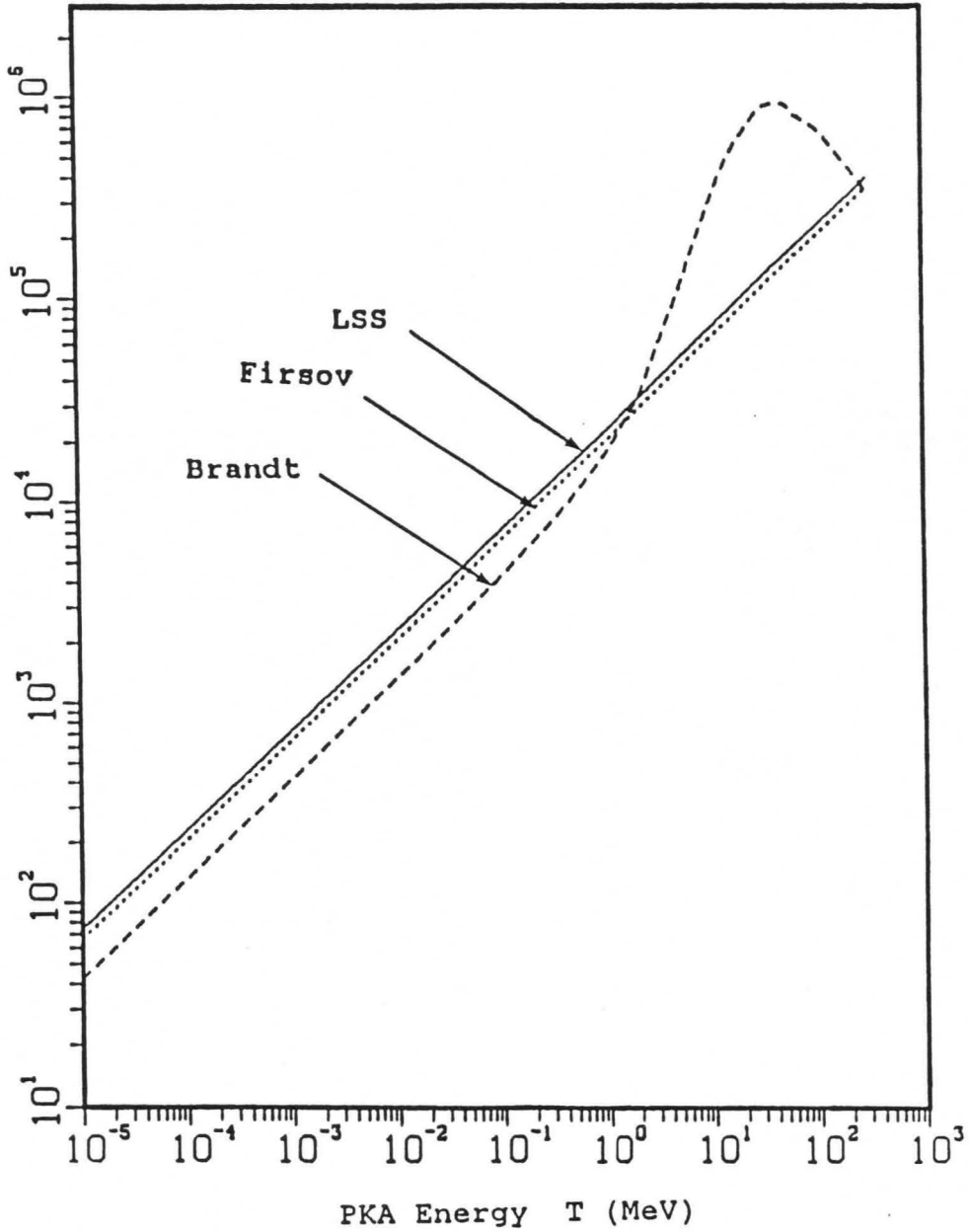


FIGURE 6. Electronic stopping power of copper for copper ions based on the LSS, Firsov, and Brandt theories

or the case of  $Z_1=Z_2=Z_c$ ,  $S_{e,F}$  in terms of  $S_{e,L}$  is

$$S_{e,F} = 1.564 (Z_1)^{-1/6} S_{e,L} \quad (84)$$

and therefore

$$k_F = 1.564 (Z_1)^{-1/6} k_L \quad (85)$$

For the case of Cu-Cu interactions,  $Z_c=29$ , and equation (61) gives  $k_L=0.157$ . Then, (85) gives  $k_F=0.140$ . The resulting  $T_{\text{dam}}$  is tabulated as a function of  $T$  in the second column of table 1.

To test the validity of the assumptions, the expression

$$T_{\text{dam}}(T') = \frac{T'}{1+k_F g(\varepsilon)} \quad (86)$$

was substituted in the integral on the right-hand side of (80). A numerical integration was then performed using 16-point Gaussian quadrature [41]. Calculations were carried out for identical projectile and struck copper atoms with atomic mass 63.546 amu and charge number 29 and for PKA energies in the range of 50 eV to 600 keV.

In the evaluation of the integral in (80), nuclear collision parameters,  $\sigma_T'(T, T')$  and  $S_n(T)$ , were expressed in terms of dimensionless quantities according to LSS theory. The differential scattering cross section  $\sigma_T'$  is given in

TABLE 1. Damage energies for copper PKAs in copper for the Firsov theory (as calculated from equation (86) and deduced from equation (80) by numerical integration using (86) as the starting function  $T_{\text{dam}}(T')$ )

PKA energy T (keV)	Damage energy from (80) $T_{\text{dam}}$ (keV)	Damage energy from (86) $T_{\text{dam}}$ (keV)
0.05	0.0445	0.0447
0.08	0.0706	0.0709
0.10	0.0879	0.0883
0.30	0.2578	0.2589
0.50	0.4246	0.4262
0.80	0.6714	0.6737
1.00	0.8343	0.8370
3.00	2.4231	2.4272
5.00	3.9673	3.9718
8.00	6.2347	6.2369
10.00	7.7211	7.7213
20.00	14.9480	14.9279
30.00	21.9141	21.8737
40.00	28.6762	28.6235
50.00	35.2703	35.2106
60.00	41.7185	41.6561
70.00	48.0385	47.9747
80.00	54.2414	54.1774
90.00	60.3347	60.2731
100.00	66.3248	66.2687
150.00	94.9638	94.9276
200.00	121.6654	121.7151
250.00	146.6993	146.9353
300.00	170.2797	170.7966
350.00	192.5514	193.4553
400.00	213.6544	215.0349
450.00	233.6921	235.6363
500.00	252.7746	255.3442
550.00	270.9856	274.2312
600.00	288.3765	292.3599

terms of  $\sigma_t$  by (see, (10) and (11))

$$\sigma_{T'}' = \sigma_t'(dt/dT') = (\pi/8)(a_L/T_L)^2 t^{-3/2} T (M_2/M_1) f(t^{1/2}) \quad (87)$$

Similarly, the nuclear stopping cross section  $S_n(T)$  in terms of  $s_n(\varepsilon)$  is, as in (48)

$$S_n(T) = 4 \pi (a_L)^2 T_L s_n(\varepsilon) M_1/(M_1+M_2) \quad (88)$$

where  $T_L$  is  $Z_1 Z_2 e^2/a_L$ , as in (7).  $s_n(\varepsilon)$  and  $f(t^{1/2})$  are tabulated by Lindhard et al. for a wide range of  $\varepsilon$  and  $t^{1/2}$  [5]. In the evaluation of equations (87) and (88),  $s_n$  and  $f(t^{1/2})$  values were determined by a four-point Lagrangian interpolation routine [48] using LSS's tabulated values. When  $\varepsilon$  was out of the range tabulated by LSS, the limiting functions (46) and (47) were used for large and small values, respectively. When  $t^{1/2}$  was out of the tabulated range, limiting functions were used, as described on page 33.

The results are tabulated in table 1, where the starting values of  $T_{\text{dam}}$  are shown as calculated from (86) and as deduced from the numerical double integration of (80). It is seen that the two  $T_{\text{dam}}$  values differ by less than about 1.4% over entire range of  $T$ .

Figure 6 shows that Brandt's stopping power is proportional to velocity at low energies. Deviations from proportionality are observed for energies above several

hundreds of keV. For  $Z_1=Z_2=Z_c$  and  $A_1=A_2=A_c$ , proportionality constant  $k_B$  for the Brandt electronic stopping cross section can be calculated by

$$k_B = 1.9703 \times 10^{-19} S_{e,B} (A_c Z_c)^{-1/2} v_o/v \quad (89)$$

where  $S_{e,B}$  is the Brandt electronic stopping cross section in  $\text{MeV cm}^2$ . Since  $S_{e,B}$  is proportional to velocity in the energy range of interest,  $T_{\text{dam}}(T)$  for the Brandt theory was approximated by

$$T_{\text{dam}}(T') = \frac{T'}{1+k_B g(\varepsilon)} \quad (90)$$

In the evaluation of Brandt's electronic stopping cross section, the velocity of the moving particle relative to the conduction electrons of the medium was determined by equation (70). The Fermi velocity for copper was taken to be 1.05 a.u. [44]. Then, the ionization fraction  $q$  corresponding to reduced velocity  $y_r$  was determined by the third degree polynomial interpolation using tabulated  $q$  values [9] for the case where the velocity stripping parameter  $b$  is 1.33. Using these values, effective charge fractions were determined. Stopping cross sections for protons were evaluated by the ENR approximation. Since the electron radius is 1.83 a.u. for copper [44], the scattering

function  $f_{\text{ENR}}(v_F)$  was approximated by means of the Lindhard-Winther scattering function (equation (77)). The scattering function was converted to electronic stopping cross section by equation (76). After having the effective charge fraction  $\zeta$  and stopping cross section for proton determined, the electronic stopping cross section for the moving particle was calculated according to equation (75). Then,  $k_B$  was calculated by equation (89).

The numerical double integration procedure was repeated to test the validity of the assumptions for the Brandt theory. Damage energies calculated for the Brandt theory by equation (90) and deduced from the numerical integration of equation (80) are tabulated in table 2. The results indicate fairly good agreement between the two  $T_{\text{dam}}$  values. The relative difference between them increases with energy  $T$  and is about 4% for the highest energy of 600 keV. The discrepancy increases with increasing  $T$  because of greater deviation of the stopping cross section from proportionality to the velocity, which makes equation (90) less valid.

The numerical integration was also carried out for the LSS damage energy function, equation (82).  $T_{\text{dam}}$  values calculated from (82) and deduced from the numerical integration of (80) are tabulated in table 3. The maximum difference between the two  $T_{\text{dam}}$  values is about 2%.



TABLE 2. Damage energies for copper PKAs in copper for the Brandt theory (as calculated from equation (90) and deduced from equation (80) by numerical integration using (90) as the starting function  $T_{\text{dam}}(T')$ )

PKA energy T (keV)	Damage energy from (80) $T_{\text{dam}}$ (keV)	Damage energy from (90) $T_{\text{dam}}$ (keV)
0.05	0.0445	0.0447
0.08	0.0736	0.0739
0.10	0.0918	0.0921
0.30	0.2711	0.2720
0.50	0.4484	0.4496
0.80	0.7118	0.7133
1.00	0.8862	0.8879
3.00	2.6001	2.6017
5.00	4.2829	4.2806
8.00	6.7623	6.7584
10.00	8.4082	8.3898
20.00	16.4440	16.3774
30.00	24.2724	24.1302
40.00	31.9309	31.7175
50.00	39.4469	39.1571
60.00	46.8370	46.4646
70.00	54.1153	53.6507
80.00	61.2898	60.7237
90.00	68.3653	67.6898
100.00	75.3467	74.5542
150.00	109.0287	107.4821
200.00	140.8021	138.3242
250.00	170.8345	167.3047
300.00	199.2787	194.5833
350.00	226.2339	220.2850
400.00	251.8130	244.5150
450.00	276.0984	267.3628
500.00	299.1929	288.9203
550.00	321.1780	309.2580
600.00	342.0977	328.4380

TABLE 3. Damage energies for copper PKAs in copper for the LSS theory (as calculated from equation (82) and deduced from equation (80) by numerical integration using (82) as the starting function  $T_{\text{dam}}(T')$ )

PKA energy T (keV)	Damage energy from (80) $T_{\text{dam}}$ (keV)	Damage energy from (82) $T_{\text{dam}}$ (keV)
0.05	0.0439	0.0441
0.08	0.0697	0.0700
0.10	0.0867	0.0871
0.30	0.2535	0.2547
0.50	0.4170	0.4187
0.80	0.6585	0.6610
1.00	0.8178	0.8207
3.00	2.3677	2.3722
5.00	3.8690	3.8750
8.00	6.0691	6.0743
10.00	7.5092	7.5134
20.00	14.4890	14.4819
30.00	21.1932	21.1770
40.00	27.6834	27.6680
50.00	33.9978	33.9890
60.00	40.1600	40.1650
80.00	52.0951	52.1341
90.00	57.8882	57.9489
100.00	63.5746	63.6613
150.00	90.6506	90.8762
200.00	115.7455	116.1925
250.00	139.1537	139.9304
300.00	161.1036	162.3084
350.00	181.7510	183.4897
400.00	201.2423	203.6026
450.00	219.6868	222.7514
500.00	237.8574	241.0235
550.00	253.8574	258.4931
600.00	269.7239	275.2243

The results of damage energy calculations for copper PKAs and copper target material for the LSS, Firsov, and Brandt theories based on equations (82), (86), and (90), respectively, are compared in table 4 and figure 7. The results show that damage energies calculated by Brandt's electronic stopping cross section are the highest for all PKA energies considered in the present work, and the LSS theory gives the lowest damage energy values.

Damage efficiency values, i.e., the proportions of the incident energy resulting in displacement production, are given in table 5. As shown in figure 8, damage efficiencies decrease with increasing PKA energy. The differences between the damage efficiencies for Firsov and LSS theories and for Brandt and LSS theories increase at first with increasing energy and then decrease again. The maximum difference for Firsov and LSS is 2.8% at about 500 keV, and for Brandt and LSS it is 11.1% at about 200 keV.

In this work, the highest PKA energy considered was 600 keV. The velocity of copper atoms corresponding to this energy is  $0.065v_1$ . It is generally agreed that stopping power is proportional to velocity in the low velocity region ( $v \ll v_1$ ) [18]. Electronic stopping cross sections determined in the present work can be assumed to be proportional to velocity. This agrees with LSS and Firsov theories. However, there is not sufficient experimental information

ABLE 4. Damage energies for copper PKAs in copper calculated based on LSS, Firsov, and Brandt electronic stopping theories

PKA energy, T (keV)	Damage Energy, $T_{\text{dam}}$ (keV)		
	LSS	FIRSOV	BRANDT
0.05	0.0441	0.0447	0.0464
0.08	0.0700	0.0709	0.0739
0.10	0.0871	0.0883	0.0921
0.30	0.2547	0.2589	0.2720
0.50	0.4187	0.4262	0.4496
0.80	0.6611	0.6737	0.7133
1.00	0.8207	0.8370	0.8879
3.00	2.3722	2.4272	2.6017
5.00	3.8750	3.9718	4.2806
8.00	6.0743	6.2369	6.7584
10.00	7.5134	7.7213	8.3898
20.00	14.4819	14.9279	16.3704
30.00	21.1770	21.8737	24.1302
40.00	27.6680	28.6235	31.7175
50.00	33.9890	35.2106	39.1571
60.00	40.1650	41.6561	46.4646
70.00	46.2092	47.9747	53.6507
80.00	52.1341	54.1774	60.7237
90.00	57.9489	60.2731	67.6898
100.00	63.6613	66.2687	74.5542
150.00	90.8762	94.9276	107.4821
200.00	116.1925	121.7151	138.3242
250.00	139.9304	146.6353	167.3047
300.00	162.3084	170.7966	194.5833
350.00	183.4897	193.4553	220.2850
400.00	203.6026	215.0349	244.5150
450.00	222.7514	235.6363	267.3628
500.00	241.0235	255.3442	288.9203
550.00	258.4931	274.2312	309.2580
600.00	275.2243	292.3599	328.4380

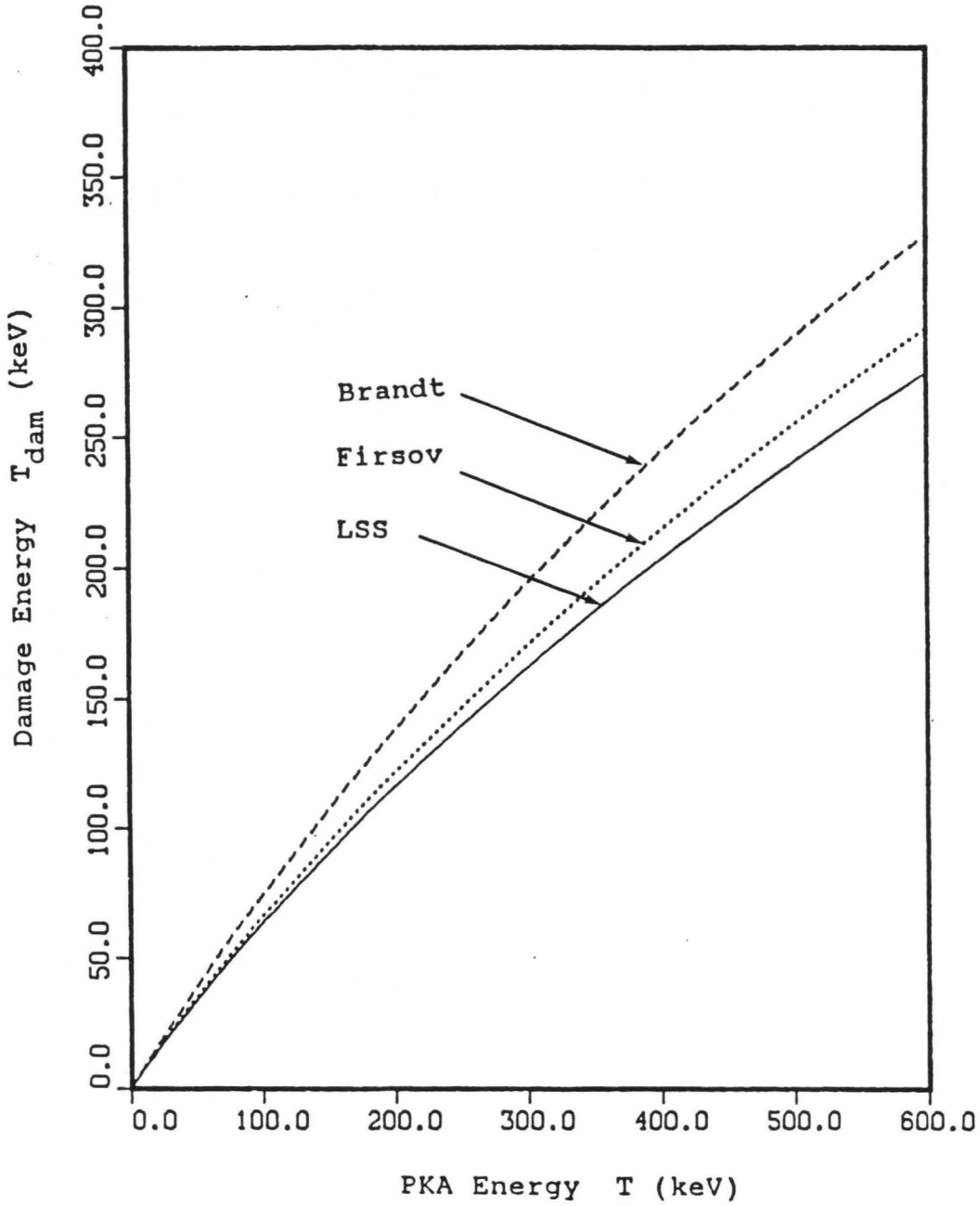


FIGURE 7. Variation of damage energies with the initial energy of PKA based on LSS, Firsov, and Brandt electronic stopping theories

TABLE 5. Damage efficiencies calculated based on LSS, Firsov, and Brandt electronic stopping theories

PKA energy, T (keV)	Damage Efficiency, $T_{\text{dam}}/T$		
	LSS	FIRSOV	BRANDT
0.05	0.8883	0.8949	0.9280
0.08	0.8754	0.8873	0.9237
0.10	0.8712	0.8835	0.9210
0.30	0.8450	0.8631	0.9066
0.50	0.8375	0.8525	0.8992
0.80	0.8263	0.8422	0.8916
1.00	0.8207	0.8370	0.8879
3.00	0.7904	0.8090	0.8672
5.00	0.7750	0.7943	0.8561
8.00	0.7593	0.7796	0.8448
10.00	0.7513	0.7721	0.8389
20.00	0.7241	0.7464	0.8185
30.00	0.7059	0.7291	0.8043
40.00	0.6917	0.7156	0.7929
50.00	0.6798	0.7042	0.7831
60.00	0.6694	0.6942	0.7744
70.00	0.6601	0.6853	0.7664
80.00	0.6516	0.6772	0.7590
90.00	0.6438	0.6697	0.7521
100.00	0.6366	0.6626	0.7455
150.00	0.6058	0.6328	0.7165
200.00	0.5809	0.6085	0.6916
250.00	0.5597	0.5877	0.6692
300.00	0.5410	0.5693	0.6486
350.00	0.5242	0.5527	0.6294
400.00	0.5090	0.5375	0.6112
450.00	0.4950	0.5236	0.5941
500.00	0.4820	0.5106	0.5778
550.00	0.4699	0.4986	0.5623
600.00	0.4587	0.4872	0.5474

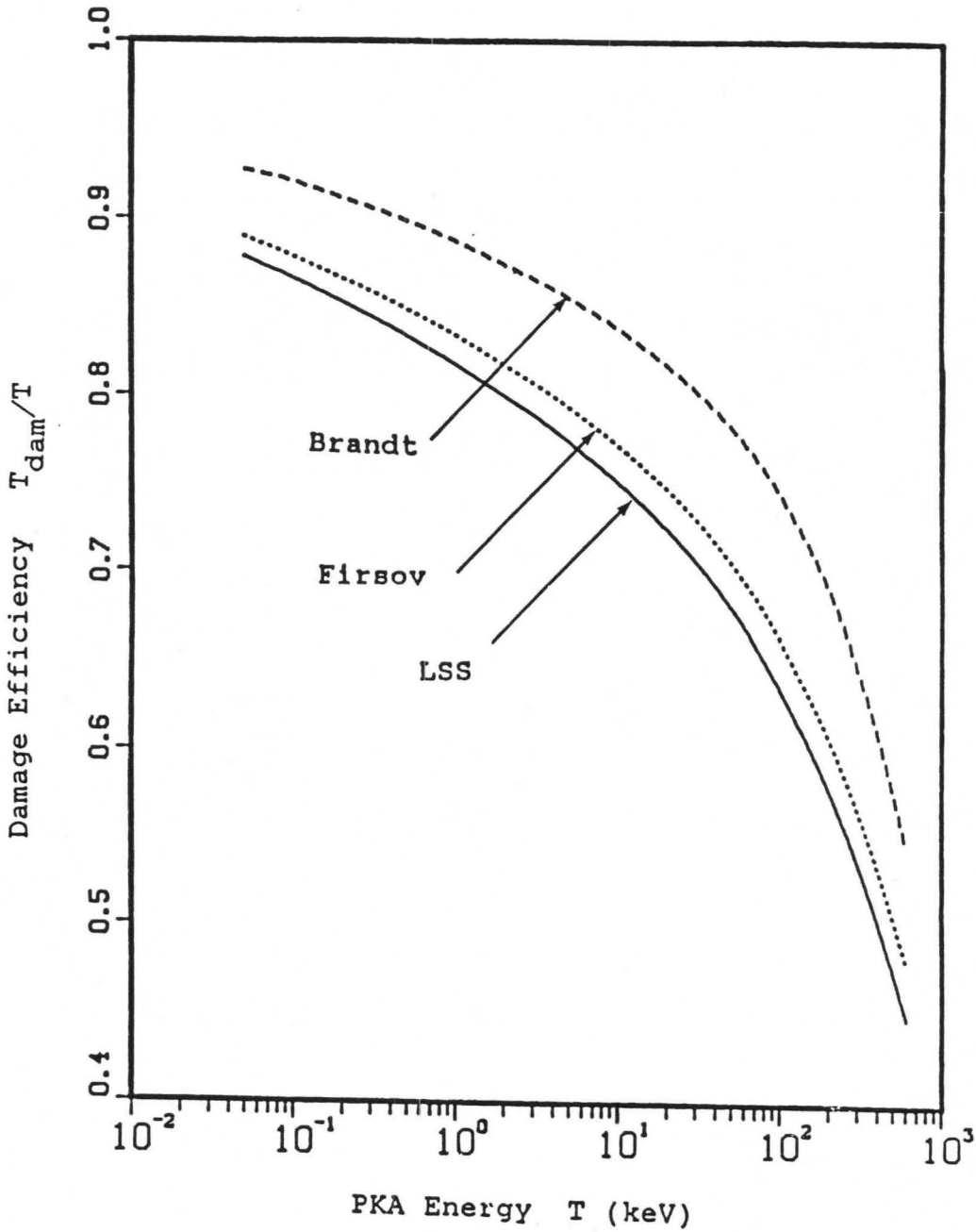


FIGURE 8. Variation of damage efficiencies with the initial energy of PKA stopping based on LSS, Firsov, and Brandt electronic stopping theories

with which to verify the magnitudes of the calculated electronic stopping cross sections. Also, for the same reason, the  $Z_1$  and  $Z_2$  oscillations could not be taken into account. For Brandt's theory, the reduced velocity  $y_r$  corresponding to 600 keV copper PKA is approximately 0.102. The reliability of Brandt and coworkers' ionization fraction,  $q$ , has been discussed by several investigators [45,46] for reduced velocities lower than 0.7. Schulz and Brandt make a comment on their theory that further studies are required in the stopping of particles at very low velocities,  $(v/v_1) < 0.2$  [49].  $v/v_1$  is 0.065 for 600 keV copper atoms. The advantage of the use of Brandt's theory is that any adjustment in the ionization fraction and stopping powers for protons can be made according to experimental observations. Thus, improvements in the prediction of low energy heavy ion stopping powers can be achieved.



## SUMMARY AND CONCLUSIONS

Theoretical models of displacement production and the stopping of energetic charged particles relevant to radiation damage studies were reviewed. Damage energies for displacement cascade formation in copper were calculated and the influence of electronic stopping theories on these calculations was analyzed.

The energy loss of moving particles in matter is primarily by nuclear and electronic collisions. Although displacement production via nuclear collisions is important at low energies, the effect of energy loss via electron excitation and ionization increases with increasing initial particle energy. Calculations showed that energy loss to electrons is about 10% of the total PKA energy at energies close to the displacement threshold energy.

Stopping theories for fast particles are well-established. Experimental observations are generally in good agreement with the theoretical predictions. However, slow heavy ions are of importance from the radiation damage point of view. In this case, accuracy in stopping parameters based on theoretical models decreases with decreasing energy. For instance, it has been reported that nuclear collision parameters based on statistically developed models have 100% deviations from experimentally deduced parameters at low energies [38]. However,

agreement is better at high velocities.

Improvements in the theories of electronic energy loss of low energetic heavy particles have been made in the last twenty-five years. Two theories, LSS and Firsov theories, have been widely used in radiation damage studies. These theories predict a velocity-proportional stopping power, which generally agrees with experimental observations in this respect. However, the accuracy of these stopping powers varies depending on the charge numbers of projectile and struck particles. These theories overpredict the stopping power at energies where stopping power is close to maximum. Brandt's theory, which is based on the effective charge concept, relates the stopping of heavy ions to the stopping of protons. The ionization, or charge fraction, of the moving ion is determined with respect to the velocity of the ion relative to the velocity of the conduction electrons of the medium. The stopping power predictions of this theory have been disputed for low energetic particles. However, it provides reasonable results for sufficiently fast particles.

In the present work, damage energy values for Firsov and Brandt theories were approximated using a function which is in the form of the one given by Lindhard et al. [3], equation (13), with different electronic stopping cross section proportionality constants. The validity of

assumptions was tested by the substitution of approximated functions into the integral equation, (80). The results show that the maximum relative differences between the two damage energy values, from the approximated function and deduced from the numerical integration, are 1.4% for the Firsov theory and 4% for the Brandt theory. The relative difference increases with increasing PKA energy. The same test resulted in a maximum difference of 2% for the LSS theory. The results also show that LSS and Firsov theories are in agreement with a 2.8% maximum difference in damage efficiencies for the considered PKA energy range. However, the Brandt theory gives considerably higher damage energies at all energies compared to LSS and Firsov theories. The maximum difference of damage efficiencies for LSS and Brandt theories is 11.1% at about 200 keV. Then, it decreases slightly at higher energies.

The accuracy of these theories is not discussed here for the specific case of Cu-Cu interaction due to the lack of experimental evidence. In general, all stopping predictions should be corrected with respect to experimental observations especially at low energies. LSS and Firsov theories can be utilized for the understanding of the average energy loss behavior of low energy charged particles. An attempt can be made to increase the accuracy in the prediction of electronic energy loss of slow

articles by adjusting some parameters in Brandt theory.  
Further work may also be done for the investigation of  
crystal structure and heat effects on stopping of ions and  
displacement production.

## BIBLIOGRAPHY

1. W. F. Sommer, L. N. Kmetyk, W. V. Green, and R. Damjanovich, *J. Nuc. Mater.* 103 and 104, 1583 (1981).
2. M. S. Wechsler, D. R. Davidson, L. R. Greenwood, and W. F. Sommer, in Effects of Radiation on Materials: Twelfth International Symposium, ASTM STP 870, edited by F. A. Garner and J. S. Perrin (American Society for Testing and Materials, Philadelphia, 1985), p. 1189.
3. J. Lindhard, V. Nielsen, M. Scharff, and P. V. Thomsen, *Mat. Fys. Medd. Dan. Vid. Selsk.* 33, No. 10 (1963).
4. J. Lindhard, M. Scharff, and H. E. Schiott, *Mat. Fys. Medd. Dan. Vid. Selsk.* 33, No. 14 (1963).
5. J. Lindhard, V. Nielsen, and M. Scharff, *Mat. Fys. Medd. Dan. Vid. Selsk.* 36, No. 10 (1968).
6. N. Bohr, *Mat. Fys. Medd. Dan. Vid. Selsk.* 18, No. 8 (1948).
7. O. B. Firsov, *Soviet Physics JEPT* 6, 534 (1958).
8. O. B. Firsov, *Soviet Physics JEPT* 9, 1076 (1959).
9. W. Brandt and M. Kitagawa, *Phys. Rev.* B25, 5631 (1982).
10. W. Brandt, *Nuc. Ins. Met.* 194, 13 (1982).
11. G. H. Kinchin and R. S. Pease, *Rep. Progr. Phys.* 18, 1 (1955).
12. M. T. Robinson and O. S. Oen, *J. Nuc. Mater.* 110, 147 (1982).
13. M. J. Norgett, M. T. Robinson, and I. M. Torrens, *Nuc. Eng. Des.* 33, 50 (1975).
14. 1982 Book of ASTM Standards, E521-82, Part 45: Nuclear Standards (American Society for Testing and Materials, Philadelphia, 1982), p. 1112.
15. H. A. Bethe, *Ann. Phys.* 5, 325 (1930).

16. F. Bloch, *Ann. Phys.* 16, 285 (1933).
17. B. Fastrup, P. Hvelplund, and C. A. Sautter, *Matt. Fys. Medd. Dan. Vid. Selsk.* 35, No. 10 (1966).
18. P. Sigmund, in Radiation Damage Process in Materials, edited by C. H. S. Dupuy (Noordhoff International Publishing Co., Leyden, 1975), p. 3.
19. J. Lindhard, *Nuc. Ins. Met.* 132, 1 (1976).
20. H. H. Andersen, J. F. Bak, H. Knudsen, and B. R. Nielsen, *Phys. Rev.* A16, 1929 (1977).
21. J. F. Ziegler, *App. Phys. Lett.* 31, 544 (1977).
22. M. D. Brown and C. D. Moak, *Phys. Rev.* B6, 90 (1972).
23. J. F. Ziegler, in Ion Implantation Science and Technology, edited by J. F. Ziegler (Academic Press, New York, 1984), p. 51.
24. C. A. Coulter, D. M. Parkin, and W. V. Green, *J. Nuc. Mater.* 67, 140 (1977).
25. I. Manning and G. P. Mueller, *Comp. Phys. Comm.* 7, 85 (1974).
26. M. T. Robinson and I. M. Torrens, *Phys. Rev.* B9, 5008 (1974).
27. F. A. Nichols, *Nuc. Tech.* 40, 98 (1978).
28. M. T. Robinson, *Phil. Mag.* 12, 741 (1965).
29. P. Sigmund, *Rad. Eff.* 1, 15 (1969).
30. D. I. R. Norris, *J. Nuc. Mater.* 40, 66 (1971).
31. K. B. Winterbon, P. Sigmund, and J. B. Sanders, *Matt. Fys. Medd. Dan. Vid. Selsk.* 37, No. 10 (1970).
32. M. T. Robinson, in Nuclear Fusion Reactors (British Nuclear Energy Society, London, 1970), p. 364.
33. J. Gittus, Irradiation Effects in Crystalline Solids (Applied Science, London, 1978) p. 9.

34. M. S. Wechsler, in Neutron Cross Sections and Technology, NBS Special Publication 299, edited by D. T. Goldman (U.S. GPO, Washington, D.C., 1968), p. 67.
35. M. T. Robinson and O. S. Oen, Phys. Rev. 132, 2385 (1963).
36. R. S. Nelson and M. W. Thompson, Phil. Mag. 8, 94 (1963).
37. M. T. Robinson in Radiation Damage in Metals, edited by N. L. Peterson and S. D. Harkness (American Society of Metals, Metals Park, 1976), p. 1.
38. W. D. Wilson, L. G. Haggmark, and J. P. Biersack, Phys. Rev. B15, 2458 (1977).
39. I. M. Torrens, Interatomic Potentials (Academic Press, New York, 1972).
40. P. Sigmund, Rev. Roum. Phys. 17, 823 (1972).
41. P. J. Davis and I. Polonsky, in Handbook of Mathematical Functions, edited by M. Abramowitz and I. A. Stegun (Dover, New York, 1970), p. 877.
42. M. T. Robinson, in Radiation-Induced Voids in Metals, edited by J. W. Corbett and L. C. Ianniello, USAEC CONF-71060 (Nat. Tech. Inf. Ser., Springfield, 1972), p. 397.
43. S. Kreussler, C. Varelass, and W. Brandt, Phys. Rev. B23, 82 (1981).
44. A. Mann and W. Brandt, Phys. Rev. 24, 4999 (1981).
45. J. F. Ziegler, J. P. Biersack, and U. Littmark, in Charge States and Dynamic Screening of Swift Ions, CONF-820131 (Oak Ridge Nat. Lab., Oak Ridge, 1983), p. 88.
46. Th. Krist and P. Mertens, Nuc. Ins. Met. Phys. Res. B2, 119 (1984).
47. C. A. Coulter, D. M. Parkin, and W. V. Green, Los Alamos National Laboratory Report No. LA-6294-MS (1976) (unpublished).

48. B. Carnahan, H. A. Luther, and J. O. Wilkes, Applied Numerical Methods (John Wiley & Sons, New York, 1969), p. 27.
49. F. Schulz and W. Brandt, in Charge States and Dynamic Screening of Swift Ions, CONF-820131 (Oak Ridge Nat. Lab., Oak Ridge, 1983), p. 188.



## ACKNOWLEDGMENTS

I would like to express my sincere thanks and appreciation to my major professor, Dr. Monroe S. Wechsler, for his valuable guidance, suggestions, and help in the accomplishment of this thesis. I would also like to express my special thanks to my wife, Nur, for her patience and encouragement during my graduate study.